

# Experimental Data of Fluid Phase Equilibria- Correlation and Prediction Models: A Review

## Authors:

Urszula Domańska

Date Submitted: 2019-07-30

Keywords: COSMO-RS, PC-SAFT, NRHB, prediction (Mod. UNIFAC, correlation GE models, Extraction, pharmaceuticals, fragrance materials, ionic liquids, limiting activity coefficients, HE, or liquid/liquid) phase equilibria, or solid, (vapor

## Abstract:

The examples of phase equilibria in binary systems, solid/liquid (SLE), liquid/liquid (LLE), vapor/liquid (VLE), as well as liquid/liquid equilibria in ternary systems mainly containing ionic liquids (ILs), or the fragrance materials, or pharmaceuticals with molecular organic solvents, such as an alcohol, or water, or hydrocarbons, are presented. The most popular correlation methods of the experimental phase equilibrium data are presented, related to the excess Gibbs free energy models such as Wilson, universal-quasichemical, UNIQUAC and non-random two-liquid model, NRTL as well as several popular theories for the modeling of the phase equilibria and excess molar enthalpy, HE in binary or ternary mixtures are presented: the group contribution method (Mod. UNIFAC) and modified UNIFAC model for pharmaceuticals and lattice theory based on non-random hydrogen bonding (NRHB). The SLE, LLE, or VLE and HE of these systems may be described by the Perturbed-Chain Polar Statistical Associating Fluid Theory (PC-SAFT), or a Conductor-like Screening Model for Real Solvents (COSMO-RS). The examples of the application of ILs as extractants for the separation of aromatic hydrocarbons from alkanes, sulfur compounds from alkanes, alkenes from alkanes, ethylbenzene from styrene, butan-1-ol from water phase, or 2-phenylethanol (PEA) from water are discussed on the basis of previously published data. The first information about the selectivity of extractant for separation can be obtained from the measurements of the limiting activity coefficient measurements by the gas-liquid chromatography technique. This review outlines the main research work carried out over the last few years on direct measurements of phase equilibria, or HE and limiting activity coefficients, the possibility of thermodynamic modeling with emphasis on recent research achievements and potential for future research.

Record Type: Published Article

Submitted To: LAPSE (Living Archive for Process Systems Engineering)

Citation (overall record, always the latest version):

LAPSE:2019.0848

Citation (this specific file, latest version):

LAPSE:2019.0848-1

Citation (this specific file, this version):

LAPSE:2019.0848-1v1

DOI of Published Version: <https://doi.org/10.3390/pr7050277>

License: Creative Commons Attribution 4.0 International (CC BY 4.0)

Review

# Experimental Data of Fluid Phase Equilibria-Correlation and Prediction Models: A Review

Urszula Domańska <sup>1,2</sup> 

<sup>1</sup> Industrial Chemistry Research Institute, Rydygiera 8, 01-793 Warsaw, Poland; Urszula.Domanska-Zelazna@ICHP.pl or Ula@ch.pw.edu.pl; Tel.: +48-22-568-2063

<sup>2</sup> Department of Physical Chemistry, Faculty of Chemistry, Warsaw Technical University, Noakowskiego 3, 00-664 Warsaw, Poland

Received: 12 April 2019; Accepted: 7 May 2019; Published: 10 May 2019



**Abstract:** The examples of phase equilibria in binary systems, solid/liquid (SLE), liquid/liquid (LLE), vapor/liquid (VLE), as well as liquid/liquid equilibria in ternary systems mainly containing ionic liquids (ILs), or the infragrance materials, or pharmaceuticals with molecular organic solvents, such as an alcohol, or water, or hydrocarbons, are presented. The most popular correlation methods of the experimental phase equilibrium data are presented, related to the excess Gibbs free energy models such as Wilson, universal-quasichemical, UNIQUAC and non-random two-liquid model, NRTL as well as several popular theories for the modeling of the phase equilibria and excess molar enthalpy,  $H^E$  in binary or ternary mixtures are presented: the group contribution method (Mod. UNIFAC) and modified UNIFAC model for pharmaceuticals and lattice theory based on non-random hydrogen bonding (NRHB). The SLE, LLE, or VLE and  $H^E$  of these systems may be described by the Perturbed-Chain Polar Statistical Associating Fluid Theory (PC-SAFT), or a Conductor-like Screening Model for Real Solvents (COSMO-RS). The examples of the application of ILs as extractants for the separation of aromatic hydrocarbons from alkanes, sulfur compounds from alkanes, alkenes from alkanes, ethylbenzene from styrene, butan-1-ol from water phase, or 2-phenylethanol (PEA) from water are discussed on the basis of previously published data. The first information about the selectivity of extrahent for separation can be obtained from the measurements of the limiting activity coefficient measurements by the gas–liquid chromatography technique. This review outlines the main research work carried out over the last few years on direct measurements of phase equilibria, or  $H^E$  and limiting activity coefficients, the possibility of thermodynamic modeling with emphasis on recent research achievements and potential for future research.

**Keywords:** (vapor; or solid; or liquid/liquid) phase equilibria;  $H^E$ ; limiting activity coefficients; ionic liquids; infragrance materials; pharmaceuticals; extraction; correlation  $G^E$  models; prediction (Mod. UNIFAC; NRHB; PC-SAFT; COSMO-RS)

## 1. Introduction

Phase equilibria is fundamental knowledge to project new technology. Ionic liquids (ILs) are new substances with specific physico-chemical properties used in catalysis, electrochemistry, new materials and with large extraction possibilities [1–8]. The most popular use of ILs in recent years is as high selectivity extrahents in the separation of aromatic/aliphatic hydrocarbons [9–13], sulfur compounds/fuels (alkanes) [14–19], alkenes from alkanes [20–24], or water/butan-1-ol [25–31], or in 2-phenylethanol/water separation [32–35].

The separation problem involves two molecular solutes to be separated and IL used as an entrainer, the solid/liquid equilibrium (SLE), or liquid/liquid equilibrium (LLE) and vapor/liquid (VLE) data in ternary systems comprising the IL and the solutes are always crucial for design and optimization of

extraction and extractive distillation stages. That is why a vast amount of experimental work has dealt with measurements of the SLE/LLE/VLE phase diagrams in ILs-based systems. The phase equilibria in systems that contain ILs has been the object of investigation in our group from many years [33–45].

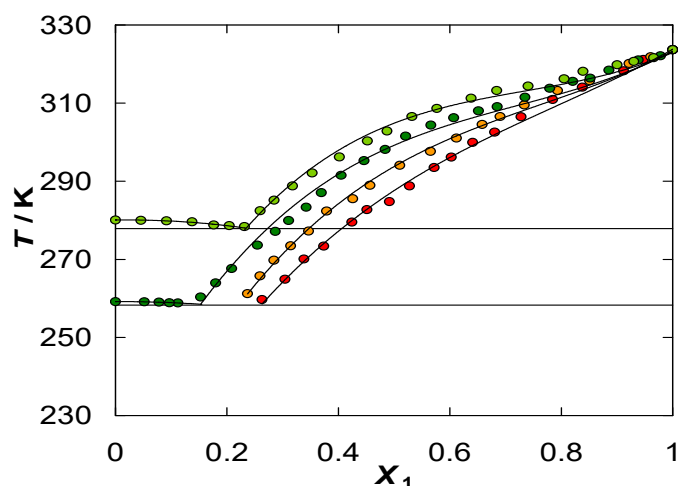
The infragrance materials are important additives in food and cosmetic technology, or as biodegradable solvents, as inhibitors in many polymerization reactions and as flavor additives in the pharmaceutical industry [46]. The SLE or LLE data provide a good tool for studying the thermodynamic behavior of many systems. Thus, many phase equilibria of infragrance materials have been measured by our group, for example, such as 2-phenylethanol, PEA (roses oil) [32–35,41,42].

Our special attention was given to the solubility of pharmaceuticals in typical solvents such as an alcohol, or water [47–52]. Research on ILs in pharmaceutical applications has been of great interest in recent years. ILs are useful for changing the kinetic in the delivery system and in general for the increasing of solubility of drugs in water [52–54].

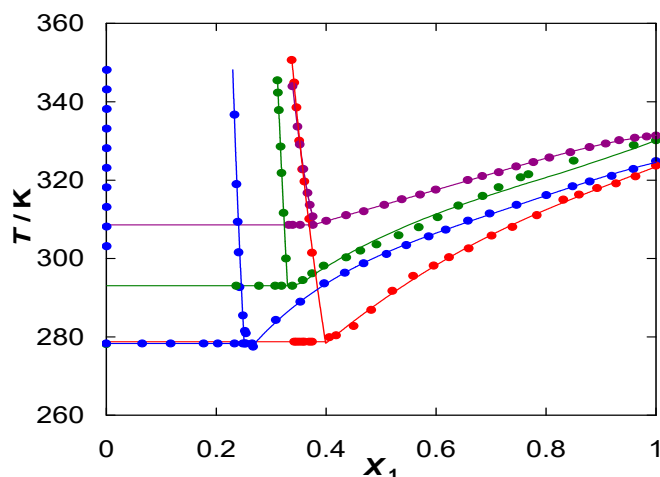
Mixtures of (IL/solvent) mainly exhibit simple eutectic systems (see Figure 1), or eutectic systems with immiscibility gap in the liquid phase with upper critical solution temperature (UCST) (see Figure 2). Strongly polar ILs reveals strong interaction with polar solvents such as water and alcohols, which is evident as complete miscibility in the liquid phase. Figure 1 presents 1-butyl-3-methyl pyridinium tosylate, {[BM<sup>3</sup>Py][TOS] (1) + 1-alcohol (2)} binary systems [55], which is typical for all ILs in mixtures with alcohols. Solubility decreases as the alkane chain length of *n*-alcohol increases.

Figure 3 represents a typical picture for the solubility of pharmaceuticals (Niflumic acid) in water and alcohol. The solubility is lower than the ideal solubility, and usually lower in water than in alcohols [50]. Solubility of organic compounds depends on the structure and polar groups in the molecule, the fusion temperature and on the enthalpy of fusion. The solubility of pharmaceuticals depends on pH, which is not predictable. Solvents used in our studies included: water and ethanol, which were typical media used for delivering of drugs; 1-octanol, which was a model compound of human cell and skin-membrane.

Only a few ILs, such as imidazolium-, or pyridinium-, or pyrrolidinium-, or piperidinium-based thiocyanate in binary systems with aromatic hydrocarbons revealed the lower critical solution temperature (LCST) behavior [56]. Most of the ILs present LLE in binary systems with water, or alcohols, as shown by the authors of [34].



**Figure 1.** Plot of the solid/liquid (SLE) in binary systems {[BM<sup>3</sup>Py][TOS] (1) + 1-alcohol (2)} (●) C<sub>4</sub>OH; (●) C<sub>6</sub>OH; (●) C<sub>8</sub>OH; (●) C<sub>10</sub>OH; Solid lines represent non-random two-liquid, NRTL equation; exptl. [55].



**Figure 2.** Plot of the SLE/liquid/liquid (LLE) in the systems of {[BMnPy][TOS] (1) + benzene (2)}: ●—{[BM<sub>4</sub>Py][TOS] (1) + benzene (2)}; ●—{[BM<sub>3</sub>Py][TOS] (1) + benzene (2)}; ●—{[HM<sub>3</sub>Py][TOS] (1) + benzene (2)}; ●—{[BMIM][TOS] (1) + benzene (2)}. Solid lines represent the NRTL equation; exptl. [55].

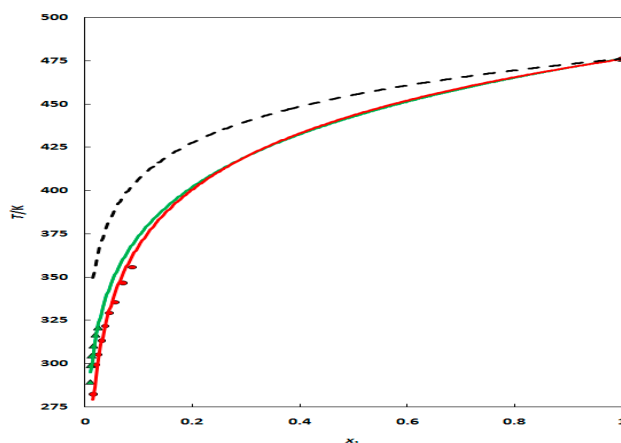


**Figure 3.** Plot of the SLE of binary system {niflumic acid +▲, ethanol, or ●, 1-octanol}; Solid lines represent the NRTL equation, dotted line presents the ideal solubility; exptl. [50].

All experimental data presented in this review, the experimental methods, the uncertainties of the measurements and the purity of the materials were published earlier in papers cited here. Some comparisons of the correlation or prediction of phase equilibria, correlation parameters and standard deviations were also presented in published papers from our group. In this review, only the examples of phase equilibria, some separation processes and useful thermodynamic methods of the correlation or prediction are reviewed in light of different process parameters and the use of ILs as modern solvents. The theories discussed in this work are used in all phase equilibrium processes, including ILs. Potential for future research in the area is highlighted.

## 2. Correlation Methods

For the correlation of the measured data, SLE, LLE, VLE and the excess molar enthalpy,  $H^E$  the excess Gibbs free energy models, such as Wilson, universal-quasichemical, UNIQUAC and NRTL are usually used [57–59]. As an example, the eutectic system may be described with these three methods

to determine the solute activity coefficients, ( $\gamma_1$ ) from the correlation equation presented below as Equation (1):

$$-\ln x_1 = \frac{\Delta_{\text{fus}}H_1}{R} \left( \frac{1}{T} - \frac{1}{T_{\text{fus},1}} \right) + \frac{\Delta_{\text{tr}}H_1}{R} \left( \frac{1}{T} - \frac{1}{T_{\text{tr},1}} \right) - \frac{\Delta_{\text{fus}}C_{p,1}}{R} \left( \ln \frac{T}{T_{\text{fus},1}} + \frac{T_{\text{fus},1}}{T} - 1 \right) + \ln \gamma_1 \quad (1)$$

where  $x_1$ ,  $\gamma_1$ ,  $\Delta_{\text{fus}}H_1$ ,  $\Delta_{\text{fus}}C_{p,1}$ ,  $T_{\text{fus},1}$ ,  $\Delta_{\text{tr}}H_1$  and  $T_{\text{tr},1}$ ,  $T$  is the mole fraction, activity coefficient, enthalpy of melting, heat capacity at melting temperature, melting temperature, enthalpy of the  $\alpha/\beta$  phase transition, transition temperature and the equilibrium temperature, respectively. The parameters of the equations are funded by an optimization technique:

$$\Omega = \sum_{i=1}^n \left[ (T_i)^{\text{exp}} - (T_i(x_1P_1, P_2))^{\text{cal}} \right]^2 \quad (2)$$

where  $\Omega$  is the objective function,  $n$  the number of experimental points, and  $(T_i)_{\text{exp}}$  and  $(T_i)_{\text{cal}}$ , are the experimental and calculated equilibrium temperature, respectively.  $P_1$  and  $P_2$  are the model parameters. The deviations are described by the root-mean-square deviation of temperature:

$$\sigma_T = \left( \sum_{i=1}^n \frac{((T_i)^{\text{exp}} - (T_i)^{\text{cal}})^2}{n-2} \right)^{1/2} \quad (3)$$

The volume parameter  $r$  and surface parameter  $q$  in the UNIQUAC equation were described as follows:

$$r_i = 0.02981V_m \quad (4)$$

$$q_i = \frac{(Z-2)r_i}{Z} + \frac{2(1-l_i)}{Z} \quad (5)$$

where  $V_m$ —molar volume of component  $i$  at temperature  $T = 298.15$  K,  $Z$  is the coordination number ( $Z = 10$ ), and  $l_i$  is the bulk factor ( $l_i = 0$  for the linear molecules).

The NRTL model is usually used for the LLE correlation in binary systems [59]:

$$\frac{G^E}{RT} = x_1x_2 \left[ \frac{\tau_{21}G_{21}}{x_1 + x_2G_{21}} + \frac{\tau_{12}G_{12}}{G_{12}x_1 + x_2} \right] \quad (6)$$

where:

$$\tau_{12} = (g_{12} - g_{22})/RT \quad (7)$$

$$\tau_{21} = (g_{21} - g_{11})/RT \quad (8)$$

$$G_{12} = \exp(-\alpha_{12}\tau_{12}) \quad (9)$$

$$G_{21} = \exp(-\alpha_{12}\tau_{21}) \quad (10)$$

The  $\gamma_1$  are calculated from:

$$\ln(\gamma_1) = x_2^2 \left[ \tau_{21} \left( \frac{G_{21}}{x_1 + x_2G_{21}} \right)^2 + \frac{\tau_{12}G_{12}}{(x_2 + x_1G_{12})^2} \right] \quad (11)$$

To calculate the activity coefficient from Equation (11), the objective function (OF) was used:

$$OF = \sum_{i=1}^n \{ (\Delta x_1)_i^2 + (\Delta x_1^*)_i^2 \} \quad (12)$$

where  $\Delta x$  or  $\Delta x^*$  (in the second phase) is the difference:

$$\Delta x = x_{\text{cal.}} - x_{\text{exp.}} \quad (13)$$

The deviation from experimental points in mole fractions is expressed as:

$$\sigma_x = \left\{ \sum_{i=1}^n \frac{(\Delta x_1)_i^2}{n-2} + \sum_{i=1}^n \frac{(\Delta x_1^*)_i^2}{n-2} \right\}^{1/2} \quad (14)$$

The NRTL equation was used for the description of the hundreds of binary SLE and LLE data of ILs, or non-ILs systems, or infragrance materials, or pharmaceutical mixtures.

The LLE in ternary systems is presented in Figure 4, as an example. The experimental tie-lines for extraction water/butan-1-ol [26] were fitted by the NRTL model [59].

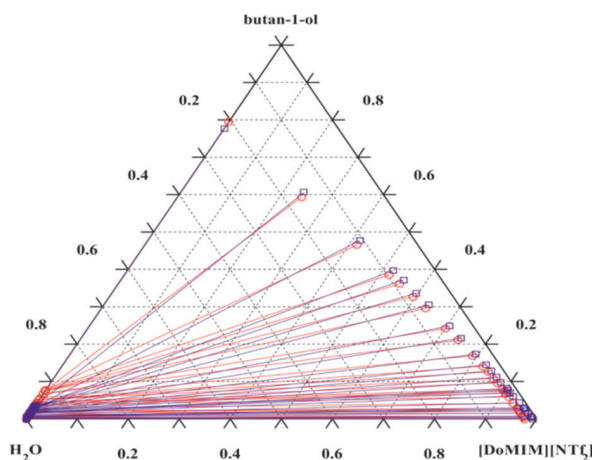


**Figure 4.** Experimental tie lines of the system  $\{[\text{DoMIM}][\text{NTf}_2]\}$  (1) + butan-1-ol (2) + water (3) at  $T = 298.15 \text{ K}$ ; (○—○) experimental data in mass fraction; (□—□) NRTL correlation; exptl. [26].

The method of correlation of liquid phase in ternary systems was presented by Wales [60]. The following objective function  $F(P)$ , was used in the calculations:

$$F(P) = \sum_{i=1}^n [x_2^{\text{Iexp}} - x_2^{\text{Icalc}}(PT)]^2 + [x_3^{\text{Iexp}} - x_3^{\text{Icalc}}(PT)]^2 + [x_2^{\text{IIexp}} - x_2^{\text{IIcalc}}(PT)]^2 + [x_3^{\text{IIexp}} - x_3^{\text{IIcalc}}(PT)]^2 \quad (15)$$

where  $P$  is the parameters vector,  $x_2^{\text{Iexp}}$ ,  $x_3^{\text{Iexp}}$  and  $x_2^{\text{Icalc}}(PT)$ ,  $x_3^{\text{Icalc}}(PT)$  and  $x_2^{\text{IIexp}}$ ,  $x_3^{\text{IIexp}}$  and  $x_2^{\text{IIcalc}}(PT)$ ,  $x_3^{\text{IIcalc}}(PT)$  are the experimental and calculated mole fractions of phase I or II. The third parameter,  $\alpha_{ij}$  in the NRTL model (usually  $\alpha_{ij} = 0.2$  or  $0.3$ ) is adjusted for the best correlation between 0 and 1. The root-mean square deviation, RMSD values were expressed as:

$$\text{RMSD} = \left( \sum_i \sum_l \sum_m [x_{ilm}^{\text{exp}} - x_{ilm}^{\text{calc}}]^2 / 6k \right)^{1/2} \quad (16)$$

where  $x$  is the mole fraction and the subscripts  $i$ ,  $l$ , and  $m$  designate the component, phase, and tie-line, respectively. Using different values of parameter  $\alpha_{ij}$  for the correlation of the experimental tie-lines mole fractions, we can get the lowest values of RMSD.

All mentioned models, such as Wilson, UNIQUAC and NRTL [57–59] are well-established methods used for the correlation of the experimental data, SLE, LLE, VLE and the excess molar enthalpy,  $H^E$  and have been used for many years. They are useful in the calculation of the activity coefficients in real systems with ILs, or without ILs from the experimental data. It is always possible to use the parameters

from binary systems for the prediction of phase equilibria in the ternary systems or to extend the range of temperature. It is worth mentioning in this moment that the Wilson model is very popular and easy to use in the SLE description, but only for the systems with complete miscibility in the liquid phase.

### 3. Predictive Methods

The most convenient theories used for the modeling of the phase equilibria and  $H^E$  have been presented by us: group contribution model (Mod. UNIFAC) [61,62] and modified UNIFAC model for pharmaceuticals [63], or lattice theory based on non-random hydrogen bonding (NRHB) [64]. In many works the SLE, LLE, or VLE and  $H^E$  of ILs were described by Perturbed-Chain Polar Statistical Associating Fluid Theory (PC-SAFT) [65,66] or Conductor-like Screening Model for Real Solvents (COSMO-RS) [67].

VLE of (IL/solvent) has been measured in our laboratory with an ebulliometric method. The VLE data usually represented simple zeotropic binary mixtures. The  $H^E$  data, measured with an isothermal titration calorimeter is usually negative for the (aromatic hydrocarbon + IL) binary mixture. This is a result of interaction of solvent with the IL. The positive values are observed for alcohols, because of the breaking of hydrogen bonding in alcohol associates (see for example *N*-alkylisoquinolinium bis((trifluoromethyl)sulfonyl)imides [ $C_n$ Quin][NTf<sub>2</sub>] (where  $C_n = C_nH_{2n+1}$ ;  $n = 4, 6, 8$ ) ILs with benzene, toluene, pyridine, or butan-1-ol [68]). The VLE and  $H^E$  modeling of these systems were made using PC-SAFT theory. To get a better prediction of the phase equilibria, the parameters of pure substances have to be obtained from experimental data of pure substances such as density, or the solubility parameters. The literature values of density or  $\gamma^\infty$  of solvents were used to determine binary interaction parameters of the models. The VLE and  $H^E$  data were possible to calculate with deviations of about 4.1% of the IL mole fraction. The use of the PC-SAFT model enabled us to describe the phase behavior in a qualitative manner for many ILs with different cations [68]. The model predicted the order in which the  $H^E$  of aromatic hydrocarbon in the IL decreases, including the number of carbon atoms of alkyl substituent in benzene ring, or in cation of the IL [68].

To have the possibility to choose the IL as selective solvent in separation process, the knowledge of the phase equilibrium behavior, or  $H^E$  is fundamental. Several modern thermodynamic models have been used for the prediction of phase equilibrium and  $H^E$  in recent years [69]. In particular, accurate predictions of the VLE and LLE with PC-SAFT [65,66] and soft-SAFT [70,71] for systems with [NTf<sub>2</sub>]-based ILs and hydrocarbon, or alcohol, or water have been demonstrated very recently.

Thus, the modeling of mixtures with ILs is important. The modeling allows us to understand the interactions in the solution and then to choose the prediction method. It is widely known that ILs have no measurable vapor pressures, which make the prediction of phase equilibria in multicomponent systems difficult. Therefore, modeling of systems with ILs needs special ideas. Many reviews of possible methods are presented in literature [69,72–74]. The statistical associating fluid theory (SAFT) and its modifications as (PC-SAFT) [65,66], (soft-SAFT) [75], (tPC-SAFT) [76,77] have become very popular for the description of the ILs solutions.

The use of general thermodynamic relations helps us to obtain the fugacity coefficient as some derivatives of  $A^{\text{res}}$  according to eqn. 17. In the original PC-SAFT, important factors are: the chain reference fluid (*hc*), dispersive interactions (*disp*) and the association in the solution (*assoc*):

$$\bar{a}^{\text{res}} \equiv \frac{A^{\text{res}}}{Nk_B T} = \bar{a}^{\text{hc}} + \bar{a}^{\text{disp}} + \bar{a}^{\text{assoc}} \quad (17)$$

where  $N$  is the number of molecules in the system and  $k_B$  is Boltzmann constant.

For the associating mixtures two parameters (per one pair of sites) describing the strength of association AB are used: the energy potential ( $\epsilon^{\text{AB}}$ ) and the volume ( $\kappa^{\text{AB}}$ ) of association AB. These parameters may be detected from pure substance properties and their mixtures, such as density, solubility parameter or vapor pressure.

It is generally known that between cations and anions of the IL the strong interaction is observed, as well as hydrogen bonding with other solvents in the solution [78–81]. For the PC-SAFT model it is necessary to assume combining rules for the cross-interaction parameters. The use of quadratic mixing rules of Lorentz–Berthelot show in many cases good results. For example, for the PC-SAFT model [65]:

$$\varepsilon_{ij} = \sqrt{\varepsilon_i \varepsilon_j} (1 - k_{ij}), \quad \sigma_{ij} = \frac{\sigma_i + \sigma_j}{2} \quad (18)$$

The expression for the calculation of the  $\gamma^\infty$  of component  $i$  (solute) in binary mixtures with component  $j$  (solvent) is as follows:

$$\gamma_i^\infty = \frac{\varphi_i^{L,\infty}}{\varphi_i^{L,0}} \quad (19)$$

where  $\varphi_i^{L,\infty}$  and  $\varphi_i^{L,0}$  are the fugacity coefficients of solute at infinite dilution (real or hypothetical) state, respectively. The expressions for  $\varphi_i^L$  can be calculated from PC-SAFT theory. Description of many phase equilibria confirmed that data of  $\gamma^\infty$ , use as experimental one or calculated from Mod. UNIFAC are important for the description.

On the other hand, COSMO-RS is a combination of unimolecular quantum chemical (QC) calculations and statistical mechanics (SM) [67,82,83]. Authors Klamt and Schüürmann of the QC basis of COSMO-RS are well known and permanently working in the field [84]. The most important property obtained from COSMO is the distribution of the density of screening charge induced at cavity surface by the surrounding conductor ( $\sigma$ ). It is important to define the ab initio calculated  $\sigma$ -profiles of all solutes and solvents existing in the solution. The chemical potentials of the components,  $\mu$  are calculated according to the expression:

$$\mu_i = \mu_i^{\text{comb}} + \int p(\sigma) \mu_s(\sigma) d\sigma + RT \ln x_i \quad (20)$$

where  $\mu_i^{\text{comb}}$  is the combinatorial contribution depending on size and shape of molecule,  $\mu_s(\sigma)$  is the chemical potential of the surface segment of screening charge density  $\sigma$ . Method of calculation both  $\mu_i^{\text{comb}}$  and  $\mu_s(\sigma)$  was published earlier [84]. Knowledge of the chemical potential enables us to calculate any phase equilibrium using known thermodynamic equations. Calculations are usually with the COSMOtherm suite (version 17.0.1; February 2017) purchased from COSMOlogic GmbH and Co. KG (Leverkusen, Germany) [85].

Coming back to the PC-SAFT calculations, the parameters (segment number  $m$ , segment diameter  $\sigma$ , dispersive interaction energy  $u/k_B$ , association energy  $\varepsilon^{\text{AB}}/k_B$  and association volume  $\kappa^{\text{AB}}$ ) for ILs must be described. They are obtained from the correlation of the experimental densities,  $\rho$  or solubility parameters,  $\delta_H$  as described earlier [86]. The PC-SAFT theory was used to the description of many pure ILs data [73,81,86–88]. The pure-fluid PC-SAFT parameters for typical molecular solvents (benzene, toluene, thiophene, pyridine and alcohols) are already described in literature [87,88].

For the binary mixtures, the parameters connected with cross-interactions (i.e., cross-dispersion and/or cross-association) have to be described. The cross-dispersive energy between IL (1) and solvent (2) can be described by the quadratic combining rules of Lorentz–Berthelot:  $u_{12} = (u_1 u_2)^{1/2} (1 - k_{12})$ ,  $\sigma_{12} = (\sigma_1 + \sigma_2)/2$ . For the cross-associating system, the cross-association energy and volume can be calculated with Wolbach–Sandler combining rules as in original PC-SAFT paper [89]. The binary interaction parameter  $k_{12}$  is usually calculated from  $\gamma_2^\infty$  of molecular solvent in the IL. The prediction of VLE, or LLE with  $k_{12}$  adjusted to  $\gamma_2^\infty$  gives quite good results. The same level of description or even better was obtained when  $\gamma_2^\infty$  was calculated from the Mod. UNIFAC model. The accuracy was much better in comparison with calculations to pure predictions based on assumption that  $k_{12} = 0$ .



For the systems, where the densities and the experimental data of  $\gamma_2^\infty$  are not available, the predicted method such as the linear solvation-energy relationship (LSER) may be used [90]. The LSER model uses many adjustable parameters from the correlation of various thermodynamic properties [90]. However, in many of our publications on phase equilibria of ILs, the  $\gamma_2^\infty$  was predicted with a Mod. UNIFAC model [91]. The comparison of the calculation based on the  $\gamma_2^\infty$ , calculated from Mod. UNIFAC, PC-SAFT-UNIFAC and with PC-SAFT pure prediction ( $k_{12} = 0$ ) together with experimental data are shown in Figure 5 for LLE data of imidazolium-based IL with alcohols [92] using the infinite dilution data of Heintz et al. [93]. Figures 6–8 show an example of the  $\gamma_2^\infty$ -based calculations compared with PC-SAFT predictions ( $k_{12} = 0$ ) and PC-SAFT-UNIFAC with experimental data of VLE of different authors [94–96]. The procedure is described as well [34].

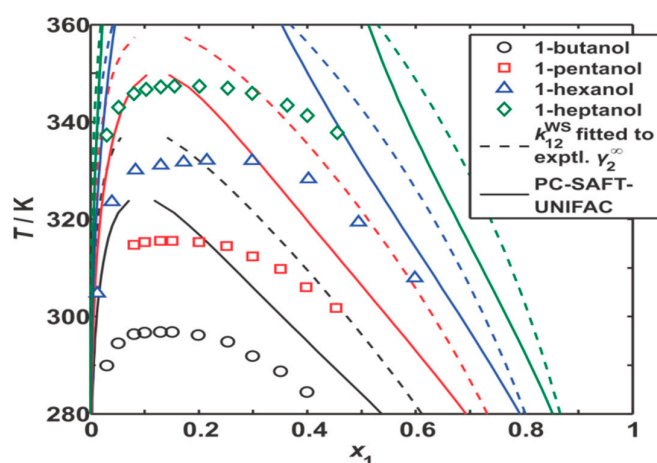


**Figure 5.** Plot of LLE of the binary systems {[BMIM][NTf<sub>2</sub>] + 1-alcohol}: prediction with—Perturbed-Chain Polar Statistical Associating Fluid Theory (PC-SAFT), and—PC-SAFT-UNIFAC. Exptl. data LLE [88]; gamma infinity data [93].

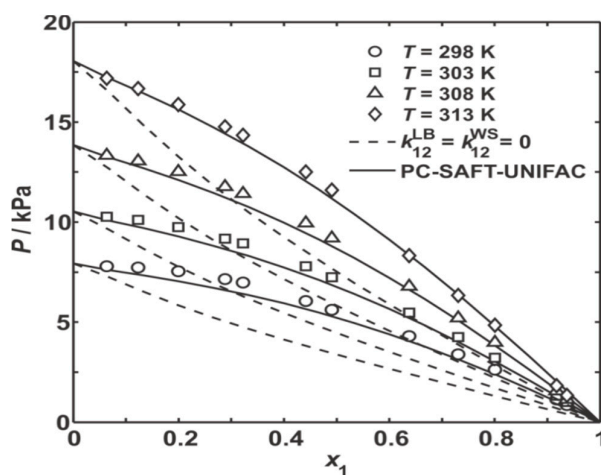


**Figure 6.** Plot of vapor/liquid (VLE) of the binary systems {[BMIM][NTf<sub>2</sub>] + ethanol} in different temperatures: prediction with—PC-SAFT, and—PC-SAFT-UNIFAC; exptl. data [94].

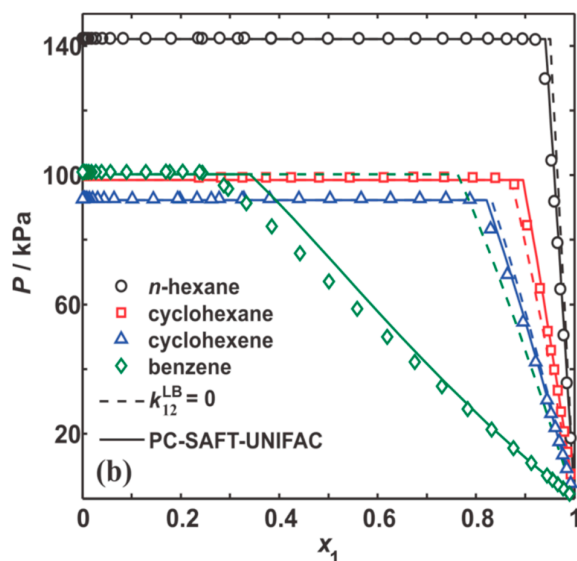


**Figure 7.** Plot of VLE of the binary systems {[EMIM][NTf<sub>2</sub>] + hydrocarbons} at  $T = 353.15$  K: prediction with—PC-SAFT, and —PC-SAFT-UNIFAC; exptl. data [95].

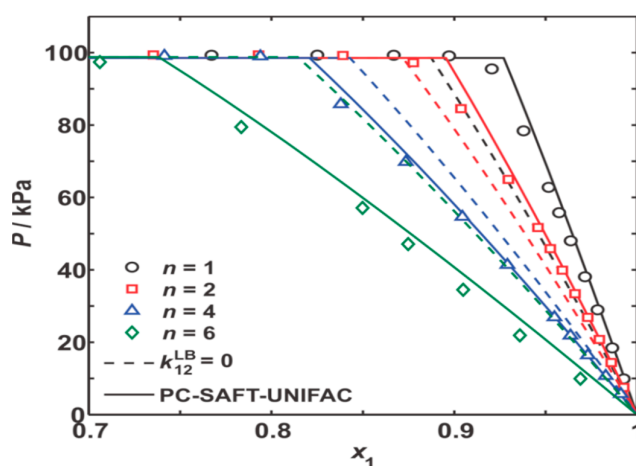


**Figure 8.** Plot of VLE of the binary systems {[C<sub>n</sub>MIM][NTf<sub>2</sub>] + cyclohexane} at  $T = 353.15$  K: prediction with—PC-SAFT, and —PC-SAFT-UNIFAC; exptl. data [95,96].

The NRHB equation of state was also used by us for the modeling of systems with ILs [97,98]. The NRHB model was used for mixtures with [NTf<sub>2</sub>]-based ILs [74], and with piperidinium-based ILs [64,70,99]. The NRHB model was used to predict binary LLE for systems containing [PMPIP][NTf<sub>2</sub>] and linear alcohols (from C<sub>5</sub>OH to C<sub>11</sub>OH) [70]. For such polar mixtures, the NRHB theory (as well as PC-SAFT,  $k_{12} = 0$ ) was not able to predict immiscibility gap in the liquid phase. It was necessary to involve the temperature dependent binary interaction parameters for the description of these binary mixtures.

In many cases, the standard quadratic mixing rules of Lorentz–Berthelot were useful in the PC-SAFT [65] and for NRHB [98]:

$$\varepsilon_{ij}^* = \sqrt{\varepsilon_i^* \varepsilon_j^*} (1 - k_{ij}) \quad (21)$$

where  $k_{ij}$  is binary interaction parameter for pair  $i$ - $j$  of components ( $k_{ij} = k_{ji}$ ). Low deviations, about 4% were obtained using the liquid density data for the pure [PMPIP][NTf<sub>2</sub>] IL in the description of LLE data in binary systems of {[PMPIP][NTf<sub>2</sub>] + alcohols (C<sub>5</sub>OH, C<sub>6</sub>OH, C<sub>7</sub>OH, C<sub>8</sub>OH, C<sub>9</sub>OH, C<sub>10</sub>OH, C<sub>11</sub>OH)} [70].

The number of segments  $r_i$  in NRHB theory was calculated from the specific volume:

$$r_i = \frac{M_i v_{sp,i}^*}{v^*} \quad (22)$$

where  $M_i$  is the molecular mass of component  $i$ . The number of external contacts is then  $q_i = s_i r_i$ .

The association term of the NRHB model,  $v^{\text{assoc}}$  is defined as:

$$v^{\text{assoc}} = \sum_{\alpha=1}^m \sum_{\beta=1}^n \frac{N_{\alpha\beta}}{rN} = \sum_{\alpha=1}^m \sum_{\beta=1}^n v_{\alpha\beta} \quad (23)$$

where  $N_{\alpha\beta}$  and  $v_{\alpha\beta}$  are average per segment and total number of complexes  $\alpha$ - $\beta$ , respectively; the number of donor groups of type  $\alpha$  in molecule of type  $i$  is  $d_i^\alpha$  and the number of acceptor groups of type  $\beta$  in molecule of type  $i$  is  $a_i^\beta$ . The parameters corresponding to the internal energy, entropy and volume change due to association of type  $\alpha$ - $\beta$ , ( $E_{\alpha\beta}^H$ ,  $S_{\alpha\beta}^H$  and  $V_{\alpha\beta}^H$ , respectively), are also introduced.

Using the presented parameters, the following equation of state can be defined:

$$\tilde{P} + \tilde{T} \left[ \ln(1 - \tilde{\rho}) - \tilde{\rho} \left( \sum_{i=1}^t \varphi_i \frac{l_i}{r_i} - v^{\text{assoc}} \right) - \frac{z}{2} \ln(1 - \tilde{\rho} + s\tilde{\rho}) + \frac{z}{2} \ln \Gamma_{00} \right] = 0 \quad (24)$$

As usual, the chemical potential has to be presented for the description of phase equilibrium:

$$\begin{aligned} \frac{\mu_i}{RT} = & \ln \frac{\varphi_i}{\omega_i r_i} - r_i \sum_{i=1}^t \varphi_i \frac{l_i}{r_i} + \ln \tilde{\rho} + r_i (\tilde{v} - 1) \ln(1 - \tilde{\rho}) \\ & - \frac{z}{2} r_i (\tilde{v} - 1 + s_i) \ln(1 - \tilde{\rho} + s\tilde{\rho}) + \frac{z}{2} s_i r_i \left[ \ln \Gamma_{ii} + \frac{\tilde{v}-1}{s_i} \ln \Gamma_{00} \right] \\ & + r_i \frac{\tilde{P}\tilde{v}}{\tilde{T}} - \frac{s_i r_i}{\tilde{T}_i} + \frac{\mu_i^{\text{assoc}}}{RT} \end{aligned} \quad (25)$$

where

$$\frac{l_i}{r_i} = \frac{z}{2} (1 - s_i) + \frac{1}{r_i} - 1 \quad (26)$$

and  $\tilde{P}$ ,  $\tilde{T}$ ,  $\tilde{T}_i$  and  $\tilde{\rho}$  are reduced state variables are defined as follows:

$$\tilde{P} = \frac{Pv^*}{\varepsilon^*}, \quad \tilde{T} = \frac{RT}{\varepsilon^*}, \quad \tilde{T}_i = \frac{RT}{\varepsilon_i^*}, \quad \tilde{\rho} = \rho v_{sp}^* \quad (27)$$

The reduced volume is defined as  $\tilde{v} = 1/\tilde{\rho}$  while the reduced density  $\tilde{\rho}$  in Equation (25) is calculated from the equation of state given in Equation (24). The formulas for the calculation of all these parameters were presented elsewhere [64,70,74,99].

Usually, description of the maximum in LLE in binary systems is not exact because in the systems with the UCST, the experimental curves are flat at the maximum [64,70,74,99].

The most popular nowadays thermodynamic models used for the prediction of the phase equilibria and  $H^E$  may be used for any binary, or ternary, or multicomponent systems including mixtures with ILs. The oldest one is group contribution method (Mod. UNIFAC) [61,62] and it is pure predictive method for phase equilibria or activity coefficient at infinite dilution. The lattice theory NRHB [64] is mainly used for non-polar systems. In many works the SLE, LLE, or VLE and  $H^E$  of binary systems are described by the PC-SAFT [65,66], but for polar compounds the experimental data are necessary to use for the description of binary interaction parameters. For such a systems we have semi-predictive method only. The COSMO-RS model [67] is popular tool with deviation of 5–10% for phase equilibria with larger deviations for systems with water and methanol.

#### 4. Separation Application Using Limiting Activity Coefficients

Much data are published in a field of separation applications using ILs; one of the most relevant is separation of aromatic/aliphatic hydrocarbons, sulfur compounds/alkanes, alkenes/alkanes, water/PEA or water/butan-1-ol or terpenes from natural sources. The best information about the selectivity of the IL used for separation can be obtained from the measurements of the  $\gamma^\infty$  by the gas–liquid chromatography technique [27,98–115].

Recently, we presented the  $\gamma^\infty$  of diverse organic solutes for new, synthesized in our laboratory ILs [100–115]. The separation of hexane/hex-1-ene, or cyclohexane/cyclohexene, or ethylbenzene/styrene was discussed with ILs presented in Table 1 [100–108], as well as separation of water/butan-1-ol with ILs listed also in Table 1 [27,109–115].

**Table 1.** Structure and names of Ionic Liquids (ILs) discussed in presented review.

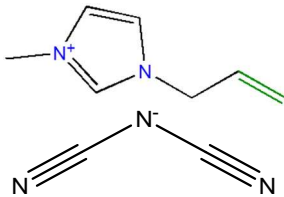
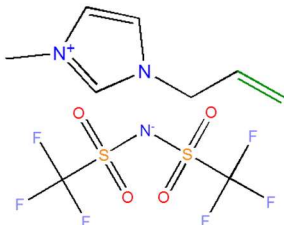
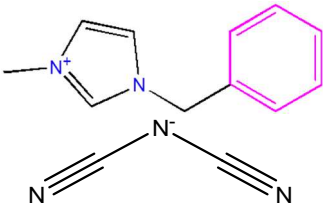
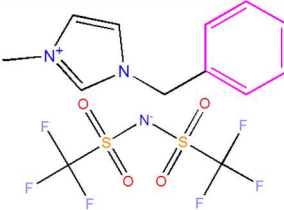
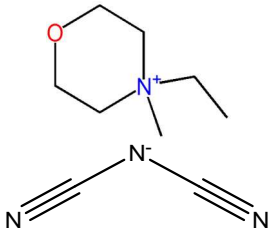
Structure	Name, Abbreviation	Ref.
Hexane/hex-1-ene, or cyclohexane/cyclohexene, or ethylbenzene/styrene separation		
	1-Allyl-3-methylimidazolium dicyanamide [AMIM][DCA]	[100]
	[AMIM][NTf <sub>2</sub> ]	[101]
	1-Benzyl-3-methylimidazolium dicyanamide, [BzMIM][DCA]	[102]
	[BzMIM][NTf <sub>2</sub> ]	[102]
	dicyanamide, [EMMOr][DCA]	[103]

Table 1. Cont.

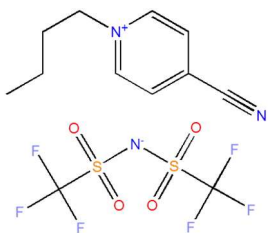
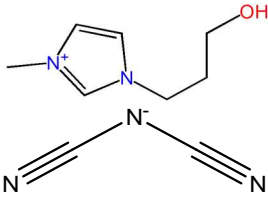
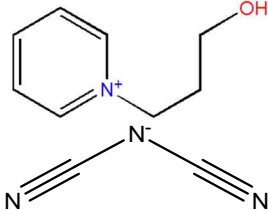
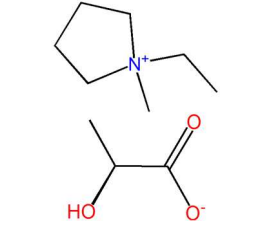
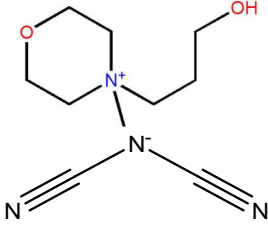
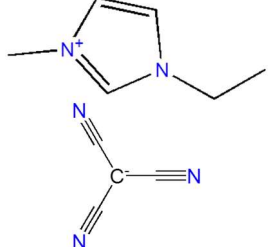
Structure	Name, Abbreviation	Ref.
	[BCN <sub>4</sub> PY][NTf <sub>2</sub> ]	[104]
	[N-C <sub>3</sub> OHMIM][DCA]	[105]
	[N-C <sub>3</sub> OHPY][DCA]	[106]
	[EMPyrr][Lac]	[107]
	[N-C <sub>3</sub> OHMor][DCA]	[105]
	[EMIM][TCM]	[109]

Table 1. Cont.

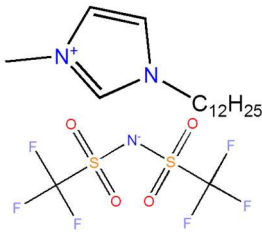
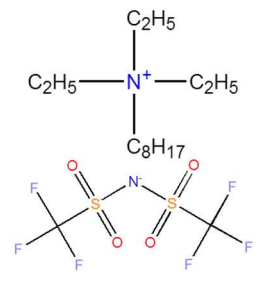
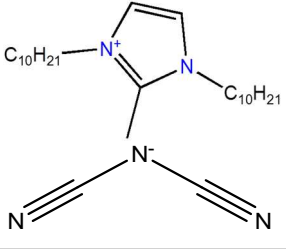
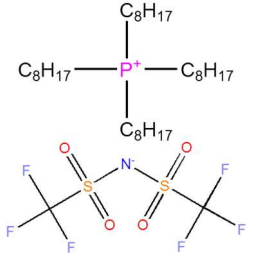
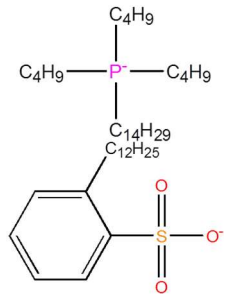
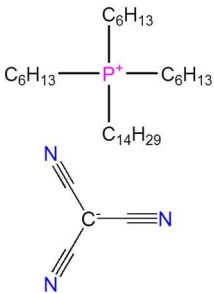
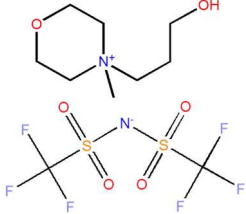
Structure	Name, Abbreviation	Ref.
Water/butan-1-ol separation		
	[DoMIM][NTf <sub>2</sub> ]	[110]
	[N <sub>8,2,2,2</sub> ][NTf <sub>2</sub> ]	[111]
	[D <sub>2</sub> MIM][DCA]	[27]
	[P <sub>8,8,8,8</sub> ][NTf <sub>2</sub> ]	[112]
	[P <sub>14,4,4,4</sub> ][DBS]	[113]

Table 1. Cont.

Structure	Name, Abbreviation	Ref.
	[P <sub>14,6,6,6</sub> ][TCM]	[114]
	[N-C <sub>3</sub> OHMMor][NTf <sub>2</sub> ]	[115]

The  $\gamma_{13}^{\infty}$  for a solute (1) partitioning between a carrier gas helium (2) and a non-volatile liquid solvent, IL (3) are determined using the gas–liquid chromatography (GLC). They are calculated from the following formula [116,117]:

$$\ln \gamma_{13}^{\infty} = \ln \left( \frac{n_3 RT}{V_N P_1^*} \right) - \frac{P_1^* (B_{11} - V_1^*)}{RT} + \frac{P_o J_2^3 (2B_{12} - V_1^{\infty})}{RT} \quad (28)$$

where  $n_3$  is the number of moles of IL,  $R$  is the gas constant,  $T$  is temperature,  $V_N$  is the net retention volume of the solute,  $P_1^*$  is the saturated vapor pressure of the solute at temperature  $T$ ,  $B_{11}$  is the second virial coefficient of pure solute,  $V_1^*$  is the molar volume of the solute,  $P_o$  is the outlet pressure,  $P_o J_2^3$  is the mean column pressure,  $B_{12}$  (the carrier gas) is the mixed second virial coefficient of the solute and helium, and  $V_1^{\infty}$  is the partial molar volume of the solute at infinite dilution (calculated as a molar volume of the solute) in the IL.

The thermodynamic constants and virial coefficients are defined in the literature [118,119] and in our earlier work [120].

The pressure correction term,  $J_2^3$ , is defined as follows [121]:

$$J_2^3 = \frac{2 (P_1/P_o)^3 - 1}{3 (P_1/P_o)^2 - 1} \quad (29)$$

The  $V_N$ , is described as:

$$V_N = (J_2^3)^{-1} U_o (t_R - t_G) \quad (30)$$

where  $t_R$  and  $t_G$  are the retention times for the solute and an unreturned gas, respectively.

Some examples of the IL, the selectivity ( $S_{12}^{\infty} = \gamma_1^{\infty}/\gamma_2^{\infty}$ ) and the capacity ( $k_2^{\infty} = 1/\gamma_2^{\infty}$ ) for four separation problems: hexane (1)/hex-1-ene (2), cyclohexane (1)/cyclohexene (2), ethylbenzene (1)/styrene (2) and water (1)/butan-1-ol (2) at  $T = 328.15$  K are presented in Tables 2–5.

**Table 2.** Selectivity and capacity at infinite dilution in hexane/hex-1-ene system at  $T = 328.15$  K.

Ionic Liquid	$S_{12}^{\infty}$	$k_2^{\infty}$
[EMMor][DCA]	2.85	0.007
[N-C <sub>3</sub> OHMIM][DCA]	2.52	0.010
[BzMIM][DCA]	2.50	0.026
[AMIM][DCA]	2.45	0.019
[EMIM][TCM]	2.35	0.045
[EMPYR][Lac]	2.24	0.020
[BCN <sub>4</sub> PY][NTf <sub>2</sub> ]	2.13	0.074
[AMIM][NTf <sub>2</sub> ]	1.94	0.094
[BzMIM][NTf <sub>2</sub> ]	1.90	0.108

**Table 3.** Selectivity and capacity at infinite dilution in cyclohexane/cyclohexene system at  $T = 328.15$  K.

Ionic Liquid	$S_{12}^{\infty}$	$k_2^{\infty}$
[N-C <sub>3</sub> OHMMor][DCA]	3.98	0.251
[EMMor][DCA]	3.04	0.329
[N-C <sub>3</sub> OHPI][DCA]	2.79	0.359
[N-C <sub>3</sub> OHMIM][DCA]	2.64	0.379
[BzMIM][DCA]	2.46	0.406
[BzMIM][NTf <sub>2</sub> ]	1.77	0.565

**Table 4.** Selectivity and capacity at infinite dilution in ethylbenzene/styrene system at  $T = 328.15$  K.

Ionic Liquid	$S_{12}^{\infty}$	$k_2^{\infty}$
[N-C <sub>3</sub> OHMMor][DCA]	2.55	0.097
[N-C <sub>3</sub> OHMIM][DCA]	2.38	0.160
[EMMor][DCA]	2.32	0.152
[N-C <sub>3</sub> OHPI][DCA]	2.27	0.138
[AMIM][DCA]	2.19	0.242
[BzMIM][DCA]	2.16	0.322
[EMIM][TCM]	2.01	0.474
[BCN <sub>4</sub> PY][NTf <sub>2</sub> ]	1.85	0.694
[AMIM][NTf <sub>2</sub> ]	1.75	0.629
[BzMIM][NTf <sub>2</sub> ]	1.71	0.758

**Table 5.** Selectivity and capacity at infinite dilution in water/butan-1-ol system at  $T = 328.15$  K.

Ionic Liquid	$S_{12}^{\infty}$	$k_2^{\infty}$
[P <sub>8,8,8,8</sub> ][NTf <sub>2</sub> ]	5.75	0.781
[P <sub>14,6,6,6</sub> ][TCM]	4.53	2.30
[P <sub>14,4,4,4</sub> ][DBS]	3.77	5.29
[DoMIM][NTf <sub>2</sub> ]	2.76	0.637
[N <sub>8,2,2,2</sub> ][NTf <sub>2</sub> ]	2.46	0.515
[N-C <sub>3</sub> OHMMor][NTf <sub>2</sub> ]	0.44	0.326

The selectivity,  $S_{12}^{\infty}$  and the capacity  $k_2^{\infty}$  at infinite dilution for the chosen ILs in the discussed separation problems were compared to the best in the literature data, which are shown as grey points in Figures 9–12.



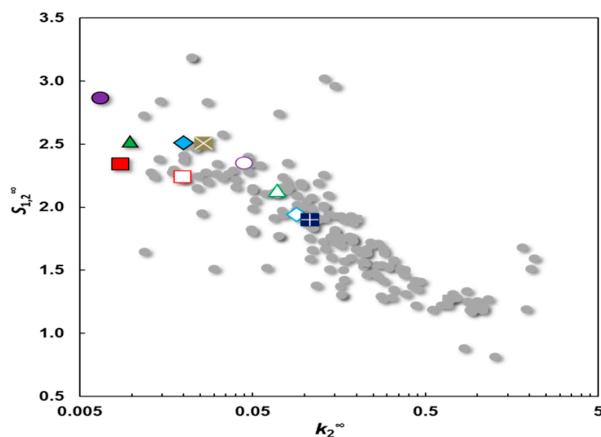


**Figure 9.** Selectivity,  $S_{12}^{\infty}$  versus capacity,  $k_2^{\infty}$  for investigated ionic liquids in comparison with other ILs from literature data for hexane/hex-1-ene system at  $T = 328.15$  K: (●) [EMMOR][DCA]; (■) [N-C<sub>3</sub>OH<sub>2</sub>PY][DCA]; (▲) [N-C<sub>3</sub>OHMIM][DCA]; (◆) [AMIM][DCA]; (⊗) [BzMIM][DCA]; (○) [EMIM][TCM]; (□) [EMPyrr][Lac]; (△) [BCN<sub>4</sub>PY][NTf<sub>2</sub>]; (◇) [AMIM][NTf<sub>2</sub>]; (■) [BzMIM][NTf<sub>2</sub>].

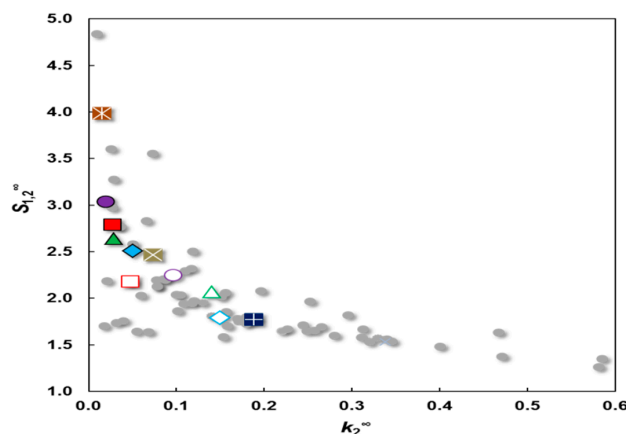


**Figure 10.** Selectivity,  $S_{12}^{\infty}$  versus capacity,  $k_2^{\infty}$  for investigated ionic liquids in comparison with other ILs from literature data for cyclohexane/cyclohexene system at  $T = 328.15$  K: (⊗) [N-C<sub>3</sub>OHMMor][DCA]; (●) [EMMOR][DCA]; (■) [N-C<sub>3</sub>OH<sub>2</sub>PY][DCA]; (▲) [N-C<sub>3</sub>OHMIM][DCA]; (◆) [AMIM][DCA]; (⊗) [BzMIM][DCA]; (○) [EMIM][TCM]; (□) [EMPyrr][Lac]; (△) [BCN<sub>4</sub>PY][NTf<sub>2</sub>]; (◇) [AMIM][NTf<sub>2</sub>]; (■) [BzMIM][NTf<sub>2</sub>].

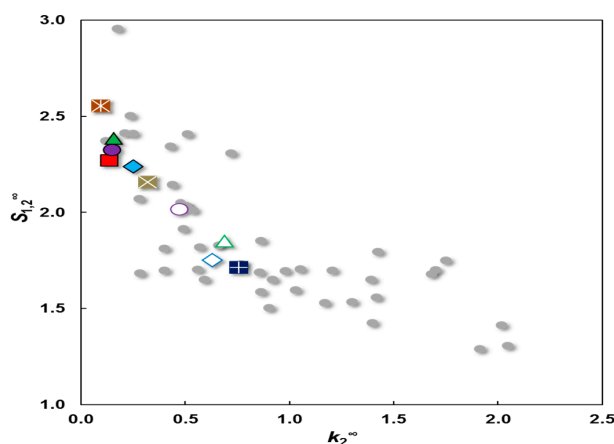


**Figure 11.** Selectivity,  $S_{12}^{\infty}$  versus capacity,  $k_2^{\infty}$  for investigated ionic liquids in comparison with other ILs from literature data for ethylbenzene/styrene system at  $T = 328.15$  K: (⊗) [N-C<sub>3</sub>OHMMor][DCA]; (●) [EMMOR][DCA]; (■) [N-C<sub>3</sub>OH<sub>2</sub>PY][DCA]; (▲) [N-C<sub>3</sub>OHMIM][DCA]; (◆) [AMIM][DCA]; (⊗) [BzMIM][DCA]; (○) [EMIM][TCM]; (□) [EMPyrr][Lac]; (△) [BCN<sub>4</sub>PY][NTf<sub>2</sub>]; (◇) [AMIM][NTf<sub>2</sub>]; (■) [BzMIM][NTf<sub>2</sub>].

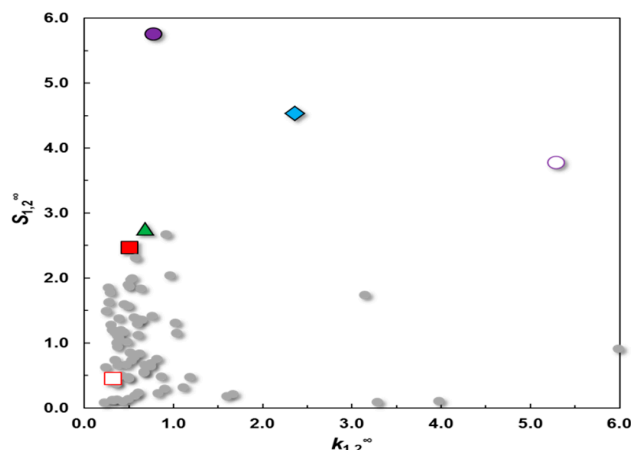


**Figure 12.** Selectivity,  $S_{12}^{\infty}$  versus capacity,  $k_{1,2}^{\infty}$  for investigated ionic liquids in comparison with other ILs from literature data for water/butan-1-ol system at  $T = 328.15$  K: (●)  $[P_{8,8,8,8}][NTf_2]$ ; (■)  $[N_{8,2,2,2}][NTf_2]$ ; (▲)  $[DoMIM][NTf_2]$ ; (◆)  $[P_{14,6,6,6}][TCM]$ ; (○)  $[P_{14,4,4,4}][DBS]$ ; (□)  $[N-C_3OHMMor][NTf_2]$ .

The largest value of selectivity for hexane/hex-1-ene separation ( $S_{12}^{\infty} = 2.85$ ) with a very low capacity ( $k_2^{\infty} = 0.007$ ) was presented by  $[EMMor][DCA]$  (see Table 2 [103]) and the lowest selectivity was observed for  $[BzMIM][NTf_2]$  ( $S_{12}^{\infty} = 1.90$ ) with large capacity ( $k_2^{\infty} = 0.108$ ) (see Table 2 [102]). Similar results are for cyclohexane/cyclohexene separation: The largest values were observed for  $[N-C_3OHMMor][DCA]$  ( $S_{12}^{\infty} = 3.98$  with capacity  $k_2^{\infty} = 0.251$ ) and  $[EMMor][DCA]$  ( $S_{12}^{\infty} = 3.04$  with capacity  $k_2^{\infty} = 0.329$ , see Table 3 [103,105]). The lowest selectivity was presented by the  $[BzMIM][NTf_2]$  ( $S_{12}^{\infty} = 1.77$ ) with the largest capacity ( $k_2^{\infty} = 0.565$ ) (see Table 3 [102]).

The largest values for ethylbenzene/styrene were observed for  $[N-C_3OHMMor][DCA]$  ( $S_{12}^{\infty} = 2.55$  with capacity  $k_2^{\infty} = 0.097$ ) and  $[N-C_3OHMIM][DCA]$  ( $S_{12}^{\infty} = 2.38$  with capacity  $k_2^{\infty} = 0.160$ , see Table 4 [105]). The lowest selectivity was presented by the  $[BzMIM][NTf_2]$  ( $S_{12}^{\infty} = 1.71$ ) with the largest capacity ( $k_2^{\infty} = 0.758$ ) (see Table 4 [102]).

The water/butan-1-ol separation problem needs different ILs with long alkane chain substituents in the cation or anion. The best values were observed for phosphonium-based ILs, such as  $[P_{8,8,8,8}][NTf_2]$  ( $S_{12}^{\infty} = 5.75$  with capacity  $k_2^{\infty} = 0.781$ ) and  $[P_{14,6,6,6}][NTf_2]$  ( $S_{12}^{\infty} = 4.53$  with capacity  $k_2^{\infty} = 2.30$ , see Table 5 [112,114]). The lowest selectivity was presented by the  $[N-C_3OHMMor][DCA]$  ( $S_{12}^{\infty} = 0.44$ ) with capacity ( $k_2^{\infty} = 0.326$ ) at temperature  $T = 328.15$  K (see Table 5 [105]).

The literature review on the hexane/hex-1-ene separation [24] has underlined the largest selectivity obtained with the ILs with the thiocyanate anion. Very good results were obtained with 1-butyl-3-methylimidazolium thiocyanate,  $[BMIM][SCN]$  ( $S_{12}^{\infty} = 3.18$ ) [122]. This type of ILs is very promising in many other separation processes. Unfortunately, the high selectivity is usually accompanied with low capacity ( $k_2^{\infty} < 0.05$ ) [122].

As seen from Tables 2–5, proposed by us, ILs may be used in application in few petrochemical separation processes. The higher values of selectivity in the separation process cyclohexane/cyclohexene than those presented here were noted in the literature only for 1-butyl-3-methylimidazolium chloride,  $[BMIM][Cl]$  [123]. The large selectivities for the ethylbenzene/styrene separation process were obtained with  $[BMIM][Cl]$  [123],  $[BMIM][MeSO_4]$  [124],  $[BMIM][BF_4]$  [125],  $[AMIM][BF_4]$  [126] and  $[BMPY][DCA]$  [127].

It has been shown that using a simple experimental method, such as measurements of limiting activity coefficients using the gas–liquid chromatography technique [27,98–115] it is possible to determine the selectivity and capacity of any extractant, including IL. It was also shown that ILs are very good, high selective new solvents for different separation problems. The results obtained with ILs are always better than those obtained with popular organic solvents.

## 5. Separation in Ternary LLE Using COSMO-RS

The second experimental method of determining the selectivity of the separation is the measurement of the ternary LLE data [24,34,35,39]. The possibility of prediction of ternary LLE with COSMO-RS was presented by us in many works [128–130].

COSMO-RS was used by us for calculating LLE phase diagrams in ternary systems of {IL+PEA+water} [130]. The PEA/water selectivity was calculated. The calculated selectivities and LLE equilibrium data enable us to make a selection of IL for extraction of PEA from aqueous solutions.

In all works, the conformations of molecules were generated and optimized using COSMOconf [85] and TURBOMOLE utilities [131–135].

Representative data on the COSMO-RS predicted vs. experimental LLE phase diagrams are shown in Figure 13. The ternary LLE experimental tie-lines are presented in the systems: {[EMIM][NTf<sub>2</sub>] + hexane + hex-1-ene} [21], {[C<sub>8</sub>iQuin][NTf<sub>2</sub>] + PEA + water} [39], {[DoMIM][NTf<sub>2</sub>] + butan-1-ol + water} [26] and {[BMPYR][FAP] + thiophene + heptane} [136] in comparison with predicted values using COSMO-RS (level TZVP-COSMO) and COSMO-RS (level TZVPD-FINE).

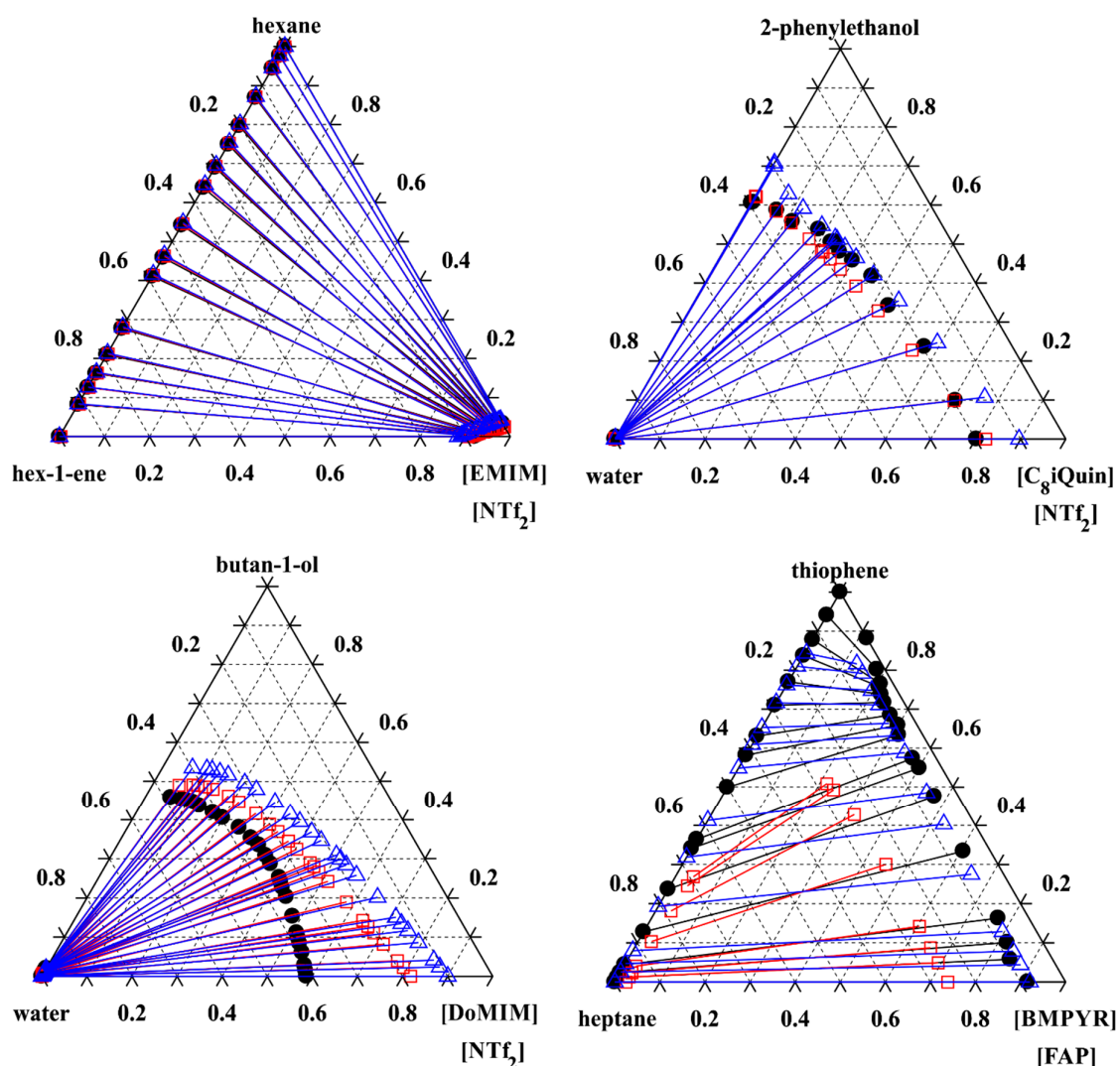


**Figure 13.** Plot of ternary LLE at  $T = 298.15$  K in the systems: {[EMIM][NTf<sub>2</sub>] + hexane + hex-1-ene} [21]; {C<sub>8</sub>iQuin][NTf<sub>2</sub>] + PEA + water} [39]; {[DoMIM][NTf<sub>2</sub>] + butan-1-ol + water} [26]; {[BMPYR][FAP] + thiophene + heptane} [136]; ●, experimental points in mole fractions, □, Conductor-like Screening Model for Real Solvents (COSMO-RS) (level TZVP-COSMO); Δ, COSMO-RS (level TZVPD-FINE).

In general, the deviation of predictions in ternary system is strongly dependent on the prediction of LLE compositions in binary mixtures. As we can see, the model correctly captures the systems of typical organic solvents with ILs. It is evidenced in Figure 13 that a great majority of ILs under study may be predicted with the COSMO-RS model.

COSMO-RS model may be useful for chemical engineering and/or thermodynamics scientists as new tool, which may suggest new applications of molecular solvents, or ILs in the separation processes. It is possible to predict the structure of new compounds, or ILs of different cations and anions for the chosen separation process. The method is shown, for example, for the prediction of the best ILs for the desulfurization of fuels [137].

## 6. Molecular Simulation as A Thermodynamic Tool

The prediction of the physico-chemical properties, such as viscosity, or density, or phase equilibria may be also studied using classical molecular dynamics (MD) simulations. The viscosities of the mixture of the IL with typical molecular solvent is always different from an ideal mixing model. Detailed analysis of the MD results reveals that different interaction between cations and anions of the IL may be shown.

Molecular simulations based on classical potentials may predict the condensed phase properties of these materials being the result of new chemical structure in the solution. MD simulations may also predict many properties and unexpected phenomena of the mixtures with the ILs. An excellent review was recently presented on the history of ILs molecular simulations, and examples of the recent use of molecular dynamics and Monte Carlo simulation in understanding the structure of ILs, the process of sorption in ILs, the immeasurable vapor pressure of ILs and the dynamics of ILs [138].

Significant advantages are obtained for example in MD simulation of the influence of soluble in water ILs on the stability of protein and enzyme structures [139]. Besides the influence of concentration of the IL, the structure, type of cation or anion can influence on distinct stabilization or denaturation mechanisms. The review in this field showed that specific ion effects, and a preferential binding model discuss protein-IL effects from a statistical mechanics perspective. The simulation of the influence of water in the self-association behavior of the IL species and recent experimental results were presented [139].

Molecular-based simulation methods similar to COSMO-RS may be useful in the prediction of structure of new ILs with planned physical properties [140]. Recently the general information about the topic of MD was presented in [140]. The calculations of thermodynamic and transport properties are presented, as well as insight into the behavior of these systems at the molecular level [140]. These information of the data base of force fields and simulation results of phase equilibria, VLE, LLE and SLE are presented [140].

Wide spectrum of the force-field data base for ILs, including 11 cations in five classes, imidazolium-, pyridinium-, pyrrolidinium-, piperidinium-, and tetraalkylammonium-based, and 12 anions, chloride, perchlorate, nitrate, tetrafluoroborate, hexafluorophosphate, thiocyanate, dicyanamide, tricyanomethanide, tetracyanoborate, bis(trifluoromethylsulfonyl)imide, triflate, and trifluoroacetate was also recently presented [141]. The parameters are primarily derived from quantum-mechanical data, with a few non-bonded parameters optimized using experimental data of density and viscosity. The force field was validated using 46 ILs with the unsigned deviations from the experimental equal to 1.4%, 12.8%, and 3.7% for density, viscosity, and isobaric heat capacity, respectively. The force field was used to analyze the interactions in terms of activation energies of viscosity and liquid structures in terms of distribution functions and free energy maps for common ILs [141].

## 7. Summary and Future Perspective

In summary, the experimental and theoretical study of some binary and ternary systems involving ILs and molecular solvents were presented. The focus was made for ILs because of enormous new applications and phase equilibria measurements and monographs about it. Ionic liquids are new

substances with specific physico-chemical properties, liquid at room temperature with no-vapor pressure and amazing solvation properties. The advantages are on the physico-chemical properties and better results in any scientific field in comparison with traditional molecular solvents and disadvantages are hygroscopy of most of them, large viscosity and the cost. Typical results of SLE, LLE and VLE, observed for system with the IL, were shown including: (1) positive deviations from Raoult's law for studied systems; (2) negative  $H^E$  of {IL + aromatic hydrocarbon} mixtures; (3) positive  $H^E$  of {IL + alcohol} mixtures. These experimental results of SLE, LLE, VLE and  $H^E$ , observed for systems with the IL, definitely show the intermolecular interaction of the IL with aromatic/aliphatic hydrocarbons or with alcohol.

The Wilson, NRTL and UNIQUAC models are popular thermodynamic models for correlation of the binary IL or any molecular solvent/solvent systems and ternary systems with or without ILs. In particular, the NRTL was confirmed to be an effective correlative model for binary and ternary LLE data. Novel modeling methodology based on PC-SAFT theory including corrections in binary systems, determined from  $\gamma^{\infty}$  data, or density of pure substances and in binary systems was demonstrated for the modeling of binary and ternary systems. It was shown that the high quality of predictions can be achieved with COSMO-RS in the case of LLE in the ternary systems studied. The use of NRHB, PC-SAFT or COSMO-RS models for the systems involving ILs is more demanding because of more difficult experimental methods in comparison with systems with typical molecular solvents. The results of any model used for the description, correlation, or prediction of the mixture depend of kind of system described (polar, non-polar, hydrogen-bonding, other specific interaction) not on the model. This work can be helpful for the development and optimization of different methods of modeling of phase equilibria (e.g., separations) and makes the process of simulation easier. In summary, this study may give some insight into new separation technologies and their thermodynamic description.

**Funding:** This research was funded by the National Science Centre (NCN) in Poland in the years 2017–2020 (UMO-2016/23/B/ST5/00145).

**Conflicts of Interest:** The authors declare no conflict of interest.

## References

1. Pârvulescu, V.; Hardacre, C. Catalysis in ionic liquids. *Chem. Rev.* **2007**, *107*, 2615–2665. [[CrossRef](#)]
2. Lewandowski, A.; Świdarska-Mocek, A. Ionic liquids as electrolytes for Li-ion batteries—An overview of electrochemical studies. *J. Power Sources* **2009**, *194*, 601–609. [[CrossRef](#)]
3. Hallet, J.P.; Welton, T. Room temperature ionic liquids: Solvents for synthesis and catalysis. *Chem. Rev.* **2011**, *11*, 3508–3676. [[CrossRef](#)] [[PubMed](#)]
4. Domańska, U. *Ionic Liquids in Chemical Analysis, Chapter 1, General Review of Ionic Liquids and Their Properties*; CRC Press, Taylor & Francis Group: Abingdon, UK, 2008; pp. 1–72.
5. Plechkova, N.V.; Seddon, K.R. Applications of ionic liquids in the chemical industry. *Chem. Soc. Rev.* **2008**, *37*, 123–150. [[CrossRef](#)] [[PubMed](#)]
6. Ibrahim, M.H.; Hayyan, M.; Hasim, M.A.; Hayyan, A. The role of ionic liquids in desulfurization of fuels: A review. *Renew. Sustain. Energy Rev.* **2017**, *76*, 1534–1549. [[CrossRef](#)]
7. Kulkarni, P.S.; Afonso, C.A.M. Deep desulfurization of diesel fuel using ionic liquids: Current status and future challenges. *Green Chem.* **2010**, *12*, 1139–1149. [[CrossRef](#)]
8. Ventura, S.P.M.; Silva, F.A.E.; Quental, M.V.; Mondal, D.; Freire, M.G.; Coutinho, J.A.P. Ionic-liquid-mediated extraction and separation processes for bioactive compounds: Past, present, and future trends. *Chem. Rev.* **2017**, *117*, 6984–7052. [[CrossRef](#)]
9. Arce, A.; Earle, M.; Katdare, S.; Rodríguez, H.; Seddon, K.S. Application of mutually immiscible ionic liquids to the separation of aromatic and aliphatic hydrocarbons by liquid extraction: A preliminary approach. *Phys. Chem. Chem. Phys.* **2008**, *10*, 2538–2542. [[CrossRef](#)]
10. Meindersma, G.W.; Hansmeier, A.R.; de Haan, A.B. Ionic liquids for aromatics extraction. Present status and future outlook. *Ind. Eng. Chem. Res.* **2010**, *49*, 7530–7540. [[CrossRef](#)]

11. Marciniak, A. Influence of cation and anion structure of the ionic liquid on extraction processes based on activity coefficients at infinite dilution. A review. *Fluid Phase Equilib.* **2010**, *294*, 213–233. [[CrossRef](#)]
12. Domańska, U.; Pobudkowska, A.; Żołek-Tryznowska, Z. Effect of an Ionic Liquid (IL) Cation on the Ternary System (IL + *p*-Xylene + Hexane) at  $T = 298.15$  K. *J. Chem. Eng. Data* **2007**, *52*, 2345–2349. [[CrossRef](#)]
13. González, E.J.; González, B.; Calvar, N.; Dominguez, Á. Application of [EMpy][ESO<sub>4</sub>] ionic liquid as solvent for the liquid extraction of xylenes from hexane. *Fluid Phase Equilib.* **2010**, *295*, 249–254. [[CrossRef](#)]
14. Kędra-Królik, K.; Mutelet, F.; Jaubert, J.-N. Extraction of Thiophene or Pyridine from n-Heptane Using Ionic Liquids. Gasoline and Diesel Desulfurization. *Ind. Eng. Chem. Res.* **2011**, *50*, 2296–2306. [[CrossRef](#)]
15. Verdía, P.; González, E.J.; Rodríguez-Cabo, B.; Tojo, E. Synthesis and characterization of new polysubstituted pyridinium-based ionic liquids: Application as solvents on desulfurization of fuel oils. *Green Chem.* **2011**, *13*, 2768–2776. [[CrossRef](#)]
16. Domańska, U.; Wlazło, M. Effect of the cation and anion of the ionic liquid on desulfurization of model fuels. *Fuel* **2014**, *134*, 114–125. [[CrossRef](#)]
17. Ahmed, O.U.; Mjalli, F.S.; Hadj-Kali, M.K.; Al-Wahaibi, T.; Al-Wahaibi, T. Measurements and prediction of ternary liquid–liquid equilibria for mixtures of IL + sulfur compound + hexadecane. *Fluid Phase Equilib.* **2016**, *421*, 16–23. [[CrossRef](#)]
18. Domańska, U.; Walczak, K.; Królikowski, M. Extraction desulfurization process of fuels with ionic liquids. *J. Chem. Thermodyn.* **2014**, *77*, 40–45. [[CrossRef](#)]
19. Durski, M.; Naidoo, P.; Ramjugernath, D.; Domańska, U. Thermodynamics and activity coefficients at infinite dilution for organic solutes in the ionic liquid 1-butyl-1-methylpyrrolidinium dicyanamide. *Fluid Phase Equilib.* **2018**, *473*, 175–182. [[CrossRef](#)]
20. Karpińska, M.; Wlazło, M.; Zawadzki, M.; Domańska, U. Liquid-liquid separation of hexane/hex-1-ene and cyclohexane/cyclohexene by dicyanamide-based ionic liquids. *J. Chem. Thermodyn.* **2018**, *116*, 299–308. [[CrossRef](#)]
21. Domańska, U.; Karpińska, M.; Wlazło, M. Separation of hex-1-ene/hexane and cyclohexene/cyclohexane compounds with [EMIM]-based ionic liquids. *Fluid Phase Equilib.* **2016**, *427*, 421–428. [[CrossRef](#)]
22. Karpińska, M.; Wlazło, M.; Domańska, U. Liquid-liquid separation of hex-1-ene from hexane and cyclohexene from cyclohexane with ionic liquids. *J. Chem. Thermodyn.* **2017**, *108*, 127–135. [[CrossRef](#)]
23. Domańska, U.; Karpińska, M.; Wlazło, M. Bis(trifluoromethylsulfonyl)imide, or dicyanamide-based ionic liquids in the liquid-liquid extraction of hex-1-ene from hexane and cyclohexene from cyclohexane. *J. Chem. Thermodyn.* **2017**, *105*, 375–384. [[CrossRef](#)]
24. Domańska, U.; Wlazło, M.; Karpińska, M. Activity coefficients at infinite dilution of organic solvents and water in the 1-butyl-3-methylimidazolium dicyanamide. A literature review of hexane/hex-1-ene separation. *Fluid Phase Equilib.* **2016**, *417*, 50–61. [[CrossRef](#)]
25. Chapeaux, A.; Simoni, L.D.; Ronan, T.S.; Stadtherr, M.A.; Brennecke, J.F. Extraction of alcohols from water with 1-hexyl-3-methylimidazolium bis(trifluoromethylsulfonyl)imide. *Green Chem.* **2008**, *10*, 1301–1306. [[CrossRef](#)]
26. Domańska, U.; Wlazło, M.; Paduszyński, K. Extraction butan-1-ol from aqueous solution using ionic liquids: An effect of cation revealed by experiments and thermodynamic models. *Sep. Purif. Technol.* **2018**, *196*, 71–81. [[CrossRef](#)]
27. Wlazło, M.; Zawadzki, M.; Domańska, U. Separation of water/butan-1-ol based on activity coefficients at infinite dilution in 1,3-didecyl-2-methylimidazolium dicyanamide ionic liquid. *J. Chem. Thermodyn.* **2018**, *116*, 316–322. [[CrossRef](#)]
28. Domańska, U.; Królikowski, M. Extraction of butan-1-ol from water with ionic liquids at  $T = 308.15$  K. *J. Chem. Thermodyn.* **2012**, *53*, 108–113. [[CrossRef](#)]
29. Hu, X.; Yu, J.; Liu, H. Liquid–Liquid Equilibria of the System 1-(2-Hydroxyethyl)-3-methylimidazolium Tetrafluoroborate or 1-(2-Hydroxyethyl)-2,3-dimethylimidazolium Tetrafluoroborate + Water + 1-Butanol at 293.15 K. *J. Chem. Eng. Data* **2006**, *51*, 691–695. [[CrossRef](#)]
30. Nann, A.; Mündges, J.; Held, C.; Verevkin, S.P.; Sadowski, G. Molecular Interactions in 1-Butanol + IL Solutions by Measuring and Modeling Activity Coefficients. *J. Phys. Chem. B* **2013**, *117*, 3173–3185. [[CrossRef](#)]
31. Marciniak, A.; Wlazło, M.; Gawkowska, J. Ternary (liquid + liquid) equilibria of {bis(trifluoromethylsulfonyl)-amide based ionic liquids + butan-1-ol + water}. *J. Chem. Thermodyn.* **2016**, *94*, 96–100. [[CrossRef](#)]

32. Sendovski, M.; Nir, N.; Fishman, A. Bioproduction of 2-phenylethanol in a biphasic ionic liquid aqueous system. *J. Agric. Food Chem.* **2010**, *58*, 2260–2265. [[CrossRef](#)] [[PubMed](#)]
33. Domańska, U.; Królikowski, M.; Zawadzki, M.; Wróblewska, A. Phase equilibrium investigation with ionic liquids and selectivity in separation of 2-phenylethanol from water. *J. Chem. Thermodyn.* **2016**, *102*, 357–366. [[CrossRef](#)]
34. Domańska, U.; Padászyński, K.; Królikowski, M.; Wróblewska, A. Separation of 2-phenylethanol from water by liquid-liquid extraction with ionic liquids—New experimental data and modelling with modern thermodynamic tools. *Ind. Eng. Chem. Res.* **2016**, *55*, 5736–5747. [[CrossRef](#)]
35. Okuniewska, P.; Domańska, U.; Więckowski, M.; Mierzejewska, J. Recovery of 2-phenylethanol from aqueous solutions of biosynthesis using ionic liquids. *Sep. Purif. Technol.* **2017**, *188*, 530–538. [[CrossRef](#)]
36. Domańska, U.; Marciniak, A. Phase behavior of 1-hexyloxymethyl-3-methylimidazolium and 1,3-dihexyloxymethylimidazolium based ionic liquids with alcohols, water, ketones and hydrocarbons: The effect of cation and anion on solubility. *Fluid Phase Equilib.* **2007**, *260*, 9–18. [[CrossRef](#)]
37. Domańska, U.; Marciniak, A.; Królikowski, M. Phase equilibria and modelling of ammonium ionic liquid, C<sub>2</sub>N<sup>+</sup>Tf<sub>2</sub><sup>-</sup>, solutions. *J. Phys. Chem. B* **2008**, *1121*, 1218–1225. [[CrossRef](#)]
38. Domańska, U.; Padászyński, K. Phase equilibria study in the binary systems (tetra-n-butylphosphonium tosylate ionic liquid + 1-alcohol, or benzene, or n-alkylbenzene). *J. Phys. Chem. B* **2008**, *112*, 11054–11059. [[CrossRef](#)]
39. Domańska, U.; Zawadzki, M.; Królikowski, M.; Lewandowska, A. Phase equilibria study of binary and ternary mixtures of {N-octylisoquinolinium bis{(trifluoromethyl)sulfonyl}imide + hydrocarbon, or an alcohol, or water}. *Chem. Eng. J.* **2012**, *181–182*, 63–71. [[CrossRef](#)]
40. Padászyński, K.; Lukoskho, E.; Królikowski, M.; Domańska, U. Measurements and equation-of-state modelling of thermodynamic properties of binary mixtures of 1-butyl-1-methylpyrrolidinium tetracyanoborate ionic liquid with molecular compounds. *J. Chem. Thermodyn.* **2015**, *90*, 317–326. [[CrossRef](#)]
41. Padászyński, K.; Okuniewski, M.; Domańska, U. “Sweet-in-Green” systems based on sugars and ionic liquids: New solubility data and thermodynamic analysis. *Ind. Eng. Chem. Res.* **2013**, *52*, 18482–18491. [[CrossRef](#)]
42. Domańska, U.; Królikowski, M.; Wlazło, M.; Więckowski, M. Extraction of 2-phenylethanol (PEA) from aqueous solution using ionic liquids: Synthesis, phase equilibrium investigation, selectivity in separation and thermodynamic models. *J. Phys. Chem. B* **2018**, *122*, 6188–6197. [[CrossRef](#)]
43. Domańska, U.; Karpińska, M.; Wiśniewska, A.; Dąbrowski, Z. Ammonium ionic liquids in extraction of bio-butanol-1-ol from water phase using activity coefficients at infinite dilution. *Fluid Phase Equilib.* **2019**, *479*, 9–16. [[CrossRef](#)]
44. Domańska, U.; Wlazło, M.; Dąbrowski, Z.; Wiśniewska, A. Ammonium ionic liquids in separation of water/butanol-1-ol using liquid-liquid equilibrium diagrams in ternary systems. *Fluid Phase Equilib.* **2019**, *485*, 23–31. [[CrossRef](#)]
45. Domańska, U.; Wlazło, M.; Karpińska, M. Separation of water/butanol with ionic liquids in ternary liquid-liquid phase equilibrium. *J. Chem. Thermodyn.* **2019**, *134*, 76–83. [[CrossRef](#)]
46. Zeitsch, K.J. *The Chemistry and Technology of Furfural and Its Many By-Products*; Elsevier: Amsterdam, The Netherlands, 2000; ISBN 0-444-50351-X.
47. Halayqa, M.; Zawadzki, M.; Domańska, U.; Plichta, A. Polymer-Ionic liquid-pharmaceutical conjugates as drug delivery systems. *J. Mol. Struct.* **2019**, *1180*, 573–584. [[CrossRef](#)]
48. Pelczarska, A.; Ramjugernat, D.; Rarey, J.; Domańska, U. Prediction of the solubility of selected pharmaceuticals in water and alcohols with a group contribution method. *J. Chem. Thermodyn.* **2013**, *62*, 118–129. [[CrossRef](#)]
49. Domańska, U.; Pobudkowska, A.; Pelczarska, A.; Żukowski, Ł. Modelling, solubility and pK<sub>a</sub> of five sparingly soluble drugs. *Int. J. Pharm.* **2011**, *403*, 115–122. [[CrossRef](#)]
50. Domańska, U.; Pobudkowska, A.; Pelczarska, A. Solubility of sparingly soluble drug derivatives of anthranilic acid. *J. Phys. Chem. B* **2011**, *115*, 2547–2554. [[CrossRef](#)]
51. Domańska, U.; Pelczarska, A.; Pobudkowska, A. Solubility and pK<sub>a</sub> determination of six structurally related phenothiazines. *Int. J. Pharm.* **2011**, *421*, 135–144. [[CrossRef](#)]
52. Halayqa, M.; Pobudkowska, A.; Zawadzki, M.; Domańska, U. Studying of drug solubility in water and alcohols using drug-ammonium ionic liquid-compounds. *Eur. J. Pharm. Sci.* **2018**, *111*, 270–277. [[CrossRef](#)]

53. Moniruzzaman, M.; Goto, M. Ionic Liquids: Future solvents and reagents for pharmaceuticals. *J. Chem. Eng. Jpn.* **2011**, *44*, 370–381. [[CrossRef](#)]
54. Bica, K.; Rijksen, C.; Nieuwenhuyzen, M.; Rogers, R.D. In search of pure liquid salt forms of aspirin: Ionic liquid approaches with acetylsalicylic acid and salicylic acid. *Phys. Chem. Chem. Phys.* **2010**, *12*, 2011–2017. [[CrossRef](#)]
55. Letcher, T.M.; Ramjugernath, D.; Tumba, K.; Królikowski, M.; Domańska, U. (Solid + Liquid) and (liquid + liquid) phase equilibria and correlation of the binary systems {N-butyl-3-methylpyridinium tosylate + water, or + an alcohol, or + a hydrocarbon}. *Fluid Phase Equilib.* **2010**, *294*, 89–97. [[CrossRef](#)]
56. Domańska, U.; Królikowska, M.; Królikowski, M. Thermodynamic phase behaviour and physico-chemical properties of the binary systems {(1-ethyl-3-methylimidazolium thiocyanate, or 1-ethyl-3-methylimidazolium tosylate + water, or + an alcohol)}. *Fluid Phase Equilib.* **2010**, *294*, 72–93. [[CrossRef](#)]
57. Wilson, G.M. Vapor-Liquid Equilibrium. XI. A New Expression for the Excess Free Energy of Mixing. *J. Am. Chem. Soc.* **1964**, *86*, 127–130. [[CrossRef](#)]
58. Abrams, D.S.; Prausnitz, J.M. Statistical Thermodynamics of Liquid Mixtures: A New Expression for the Excess Gibbs Energy of Partly or Completely Miscible Systems. *AIChE J.* **1975**, *21*, 116–128. [[CrossRef](#)]
59. Renon, H.; Prausnitz, J.M. Local compositions in thermodynamic excess functions for liquid mixtures. *AIChE J.* **1968**, *14*, 135–144. [[CrossRef](#)]
60. Walas, S.W. *Phase Equilibria in Chemical Engineering*; Butterworth Publishers: Boston, MA, USA, 1985; pp. 279–297.
61. Weidlich, U.; Gmehling, J. A modified UNIFAC model. 1. Prediction of VLE,  $h^E$ , and  $\gamma_{\infty}$ . *Ind. Eng. Chem. Res.* **1987**, *26*, 1372–1381. [[CrossRef](#)]
62. Gmehling, J.; Li, J.; Schiller, M. A modified UNIFAC model. 2. Present parameter matrix and results for different thermodynamic properties. *Ind. Eng. Chem. Res.* **1993**, *32*, 178–193. [[CrossRef](#)]
63. Moller, B. Activity of Complex Multifunctional Organic Compounds in Common Solvents. Ph.D. Thesis, Chemical Engineering, University of KwaZulu-Natal, Durban, South Africa, 2009.
64. Padászyński, K.; Domańska, U. Solubility of aliphatic hydrocarbons in piperidinium ionic liquids: Measurements and modeling in terms of perturbed-bonding-chain statistical associating fluid theory and nonrandom hydrogen-bonding theory. *J. Phys. Chem. B* **2011**, *115*, 12537–12548. [[CrossRef](#)]
65. Gross, J.; Sadowski, G. Perturbed-Chain SAFT: An Equation of State Based on a Perturbation Theory for Chain Molecules. *Ind. Eng. Chem. Res.* **2001**, *40*, 1244–1260. [[CrossRef](#)]
66. Gross, J.; Sadowski, G. Application of the Perturbed-Chain SAFT Equation of State to Associating Systems. *Ind. Eng. Chem. Res.* **2002**, *41*, 5510–5515. [[CrossRef](#)]
67. Klamt, A. *COSMO-RS: From Quantum Chemistry to Fluid Phase Thermodynamics and Drug Design*; Elsevier: Amsterdam, The Netherlands, 2005.
68. Domańska, U.; Zawadzki, M.; Królikowski, M. Heat capacity, excess molar volumes and excess dynamic viscosity of binary systems of N-octylisoquinolinium bis((trifluoromethyl)sulfonyl)imide ionic liquid. *Z. Phys. Chem.* **2013**, *227*, 217–238. [[CrossRef](#)]
69. Vega, J.F.; Vilaseca, O.; Llovel, F.; Andreu, J.S. Modeling ionic liquids and the solubility of gases in them: Recent advances and perspectives. *Fluid Phase Equilib.* **2010**, *294*, 15–30. [[CrossRef](#)]
70. Padászyński, K.; Chiyen, J.; Ramjugernath, D.; Letcher, T.M.; Domańska, U. Liquid-liquid phase equilibria of (piperidinium-based ionic liquid + an alcohol) binary systems in terms of NRHB model and PC-SAFT. *Fluid Phase Equilib.* **2011**, *305*, 43–52. [[CrossRef](#)]
71. Padászyński, K.; Domańska, U. Thermodynamic modeling of ionic liquid systems. Development and detailed overview of novel methodology based on the PC-SAFT. *J. Phys. Chem. B* **2012**, *116*, 5002–5018. [[CrossRef](#)]
72. Domańska, U.; Zawadzki, M.; Tshibangu, M.; Ramjugernath, D.; Letcher, T.M. Phase equilibria study of {N-hexylisoquinolinium bis((trifluoromethyl)sulfonyl)imide + aromatic hydrocarbons or an alcohol} binary systems. *J. Phys. Chem. B* **2011**, *115*, 4003–4010. [[CrossRef](#)]
73. Llovel, L.; Valente, E.; Vilaseca, O.; Vega, L.F. Modeling complex associating mixtures with  $[C_n\text{-mim}][\text{Tf}_2\text{N}]$  ionic liquids: Predictions from the Soft-SAFT Equation. *J. Phys. Chem. B* **2011**, *115*, 4387–4398. [[CrossRef](#)]
74. Tsiptsias, C.; Tsivintzelis, I.; Panayiotou, C. Equation-of-state modeling of mixtures with ionic liquids. *Phys. Chem. Chem. Phys.* **2010**, *12*, 4843–4851. [[CrossRef](#)]



75. Blas, F.J.; Vega, L.F. Thermodynamic behaviour of homonuclear and heteronuclear Lennard-Jones chains with association sites from simulation and theory. *Mol. Phys.* **1997**, *92*, 135–150. [[CrossRef](#)]
76. Karakatsani, E.K.; Economu, I.G. Perturbed chain-statistical associating fluid theory extended to dipolar and quadrupolar molecular fluids. *J. Phys. Chem. B* **2006**, *110*, 9252–9261. [[CrossRef](#)]
77. Karakatsani, E.K.; Kantageorgis, G.M.; Economu, I.G. Evaluation of the truncated perturbed chain-polar statistical associating fluid theory for complex mixture fluid phase equilibria. *Ind. Eng. Chem. Res.* **2006**, *45*, 6063–6074. [[CrossRef](#)]
78. Tan, S.P.; Adirama, H.; Radosz, M. Recent advances and applications of statistical associating fluid theory. *Ind. Eng. Chem. Res.* **2008**, *47*, 8063–8082. [[CrossRef](#)]
79. Shimizu, K.; Tariq, M.; Costa Gomes, M.; Rebelo, L.P.N.; Canongia Lopes, J.N.A. Assessing the dispersive and electrostatic components of the cohesive energy of ionic liquids using molecular dynamics simulations and molar refraction data. *J. Phys. Chem. B* **2010**, *114*, 5831–5834. [[CrossRef](#)] [[PubMed](#)]
80. Fernandes, A.M.; Rocha, M.A.A.; Freire, M.G.; Marrucho, I.M.; Coutinho, J.A.P.; Santos, L.M.N.B.F. Evaluation of cation–anion interaction strength in ionic liquids. *J. Phys. Chem. B* **2011**, *115*, 4033–4041. [[CrossRef](#)] [[PubMed](#)]
81. Andreu, J.S.; Vega, L.F. Modeling the solubility behavior of CO<sub>2</sub>, H<sub>2</sub>, and Xe in [Cn-mim][Tf<sub>2</sub>N] ionic liquids. *J. Phys. Chem. B* **2008**, *112*, 15398–15406. [[CrossRef](#)] [[PubMed](#)]
82. Klamt, A. Conductor-like screening model for real solvents: A new approach to the quantitative calculation of solvation phenomena. *J. Phys. Chem.* **1995**, *99*, 2224–2235. [[CrossRef](#)]
83. Klamt, A.; Eckert, F. COSMO-RS: A novel and efficient method for the a priori prediction of thermophysical data of liquids. *Fluid Phase Equilib.* **2000**, *172*, 43–72. [[CrossRef](#)]
84. Klamt, A.; Schüürmann, G. COSMO: A new approach to dielectric screening in solvents with explicit expressions for the screening energy and its gradient. *J. Chem. Soc. Perkin Trans.* **1993**, *2*, 799–805. [[CrossRef](#)]
85. Eckert, F.; Klamt, A. *COSMOtherm (v. C3.0, Release 17.01)*; COSMOlogic GmbH & Co. KG: Leverkusen, Germany, 2017.
86. Domańska, U.; Okuniewska, P.; Padaszyński, K.; Królikowska, M.; Zawadzki, M.; Więckowski, M. Extraction of 2-phenylethanol (PEA) from aqueous solution using ionic liquids: synthesis, phase equilibrium investigation, selectivity in separation, and thermodynamic models. *J. Phys. Chem. B* **2017**, *121*, 7689–7698. [[CrossRef](#)]
87. Ferreira, A.R.; Freire, M.G.; Ribeiro, J.C.; Lopes, F.M.; Crespo, J.G.; Coutinho, J.A.P. An Overview of the Liquid–Liquid Equilibria of (Ionic Liquid + Hydrocarbon) Binary Systems and Their Modeling by the Conductor-like Screening Model for Real Solvents. *Ind. Eng. Chem. Res.* **2011**, *50*, 5279–5294. [[CrossRef](#)]
88. Domańska, U.; Zawadzki, M.; Padaszyński, K.; Królikowski, M. Perturbed-chain SAFT as a versatile tool for thermodynamic modeling of binary mixtures containing isoquinolinium ionic liquids. *J. Phys. Chem. B* **2012**, *116*, 8191–8200. [[CrossRef](#)]
89. Padaszyński, K.; Domańska, U. New group contribution method for prediction of density of pure ionic liquids over a wide range of temperature and pressure. *Ind. Eng. Chem. Res.* **2012**, *51*, 591–604. [[CrossRef](#)]
90. Abraham, M.H. Scales of solute hydrogen-bonding: Their construction and application to physicochemical and biochemical processes. *Chem. Soc. Rev.* **1993**, *22*, 73–85. [[CrossRef](#)]
91. Hector, T.; Gmehling, J. Present status of the modified UNIFAC model for the prediction of phase equilibria and excess enthalpies for systems with ionic liquids. *Fluid Phase Equilib.* **2014**, *371*, 82–92. [[CrossRef](#)]
92. Vale, W.R.; Rathke, B.; Will, S.; Schröer, W. Liquid–liquid phase behavior of solutions of 1-octyl- and 1-decyl-3-methylimidazolium bis(trifluoromethylsulfonyl)imide (C<sub>8,10</sub>mimNTf<sub>2</sub>) in *n*-alkyl alcohols. *J. Chem. Eng. Data* **2010**, *55*, 2030–2038. [[CrossRef](#)]
93. Heintz, A.; Kulikov, D.V.; Verevkin, S.P. Thermodynamic properties of mixtures containing ionic liquids. 2. Activity coefficients at infinite dilution of hydrocarbons and polar solutes in 1-methyl-3-ethyl-imidazolium bis(trifluoromethyl-sulfonyl) amide and in 1,2-dimethyl-3-ethyl-imidazolium bis(trifluoromethyl-sulfonyl) amide using gas–liquid chromatography. *J. Chem. Eng. Data* **2002**, *47*, 894–899.
94. Verevkin, S.P.; Safarov, J.; Bich, E.; Hassel, E.; Heintz, A. Thermodynamic properties of mixtures containing ionic liquids: Vapor pressures and activity coefficients of *n*-alcohols and benzene in binary mixtures with 1-methyl-3-butyl-imidazolium bis(trifluoromethyl-sulfonyl) imide. *Fluid Phase Equilib.* **2005**, *236*, 222–228. [[CrossRef](#)]

95. Kato, R.; Gmehling, J. Activity coefficients at infinite dilution of various solutes in the ionic liquids [MMIM]<sup>+</sup>[CH<sub>3</sub>SO<sub>4</sub>]<sup>-</sup>, [MMIM]<sup>+</sup>[CH<sub>3</sub>OC<sub>2</sub>H<sub>4</sub>SO<sub>4</sub>]<sup>-</sup>, [MMIM]<sup>+</sup>[(CH<sub>3</sub>)<sub>2</sub>PO<sub>4</sub>]<sup>-</sup>, [C<sub>5</sub>H<sub>5</sub>NC<sub>2</sub>H<sub>5</sub>]<sup>+</sup>[(CF<sub>3</sub>SO<sub>2</sub>)<sub>2</sub>N]<sup>-</sup> and [C<sub>5</sub>H<sub>5</sub>NH]<sup>+</sup>[C<sub>2</sub>H<sub>5</sub>OC<sub>2</sub>H<sub>4</sub>OSO<sub>3</sub>]<sup>-</sup>. *Fluid Phase Equilib.* **2004**, *226*, 37–44. [[CrossRef](#)]
96. Kato, R.; Gmehling, J. Systems with ionic liquids: Measurement of VLE and  $\gamma^\infty$  data and prediction of their thermodynamic behavior using original UNIFAC, mod. UNIFAC(Do) and COSMO-RS(Ol). *J. Chem. Thermodyn.* **2005**, *37*, 603–619. [[CrossRef](#)]
97. Panayiotou, C.; Pantoula, M.; Stefanis, E.; Tsivintzelis, I.; Economou, I.G. Nonrandom hydrogen-bonding model of fluids and their mixtures. 1. Pure fluids. *Ind. Eng. Chem. Res.* **2004**, *43*, 6592–6606. [[CrossRef](#)]
98. Panayiotou, C.; Tsivintzelis, I.; Economou, I.G. Nonrandom hydrogen-bonding model of fluids and their mixtures. 2. Multicomponent mixtures. *Ind. Eng. Chem. Res.* **2007**, *46*, 2628–2636. [[CrossRef](#)]
99. Padaszyński, K.; Domańska, U. Limiting activity coefficients and gas-liquid partition coefficients of various solutes in piperidinium ionic liquids—measurements and LSER calculations. *J. Phys. Chem. B* **2011**, *115*, 8207–8215. [[CrossRef](#)]
100. Wlazło, M.; Karpkowska, J.; Domańska, U. Separation based on limiting activity coefficients of various solutes in 1-allyl-3-methylimidazolium dicyanamide ionic liquid. *Ind. Eng. Chem. Res.* **2016**, *55*, 5054–5062. [[CrossRef](#)]
101. Wlazło, M.; Karpińska, M.; Domańska, U. Thermodynamics and selectivity of separation based on activity coefficients at infinite dilution of various solutes in 1-allyl-3-methylimidazolium bis(trifluoromethylsulfonyl)imide ionic liquid. *J. Chem. Thermodyn.* **2016**, *102*, 39–47. [[CrossRef](#)]
102. Karpińska, M.; Wlazło, M.; Ramjugernath, D.; Naidoo, P.; Domańska, U. Assessment of certain ionic liquids for separation of binary mixtures based on gamma infinity data measurements. *RSC Adv.* **2017**, *7*, 7092–7107. [[CrossRef](#)]
103. Domańska, U.; Karpińska, M.; Wlazło, M. Thermodynamic study of molecular interaction-selectivity in separation processes based on limiting activity coefficients. *J. Chem. Thermodyn.* **2018**, *121*, 112–120. [[CrossRef](#)]
104. Wlazło, M.; Karpińska, M.; Domańska, U. A 1-alkylcyanopyridinium-based ionic liquid in the hexane/hex-1-ene separation. *J. Chem. Thermodyn.* **2016**, *97*, 253–260. [[CrossRef](#)]
105. Karpińska, M.; Wlazło, M.; Zawadzki, M.; Domańska, U. Separation of binary mixtures hexane/hex-1-ene, cyclohexane/cyclohexene and ethylbenzene/styrene based on gamma infinity data measurements. *J. Chem. Thermodyn.* **2018**, *118*, 244–254. [[CrossRef](#)]
106. Domańska, U.; Wlazło, M.; Karpińska, M.; Zawadzki, M. Separation of binary mixtures hexane/hex-1-ene, cyclohexane/cyclohexene and ethylbenzene/styrene based on limiting activity coefficients. *J. Chem. Thermodyn.* **2017**, *110*, 227–236. [[CrossRef](#)]
107. Domańska, U.; Karpińska, M.; Zawadzki, M. Activity coefficients at infinite dilution for organic solutes and water in 1-ethyl-1-methylpyrrolidinium lactate. *J. Chem. Thermodyn.* **2015**, *89*, 127–133. [[CrossRef](#)]
108. Domańska, U.; Karpińska, M. The use of ionic liquids for separation of binary hydrocarbons mixtures based on gamma infinity data measurements. *J. Chem. Thermodyn.* **2018**, *127*, 95–105. [[CrossRef](#)]
109. Karpińska, M.; Wlazło, M.; Domańska, U. Separation of binary mixtures based on gamma infinity data using [EMIM][TCM] ionic liquid and modelling of thermodynamic functions. *J. Mol. Liq.* **2017**, *225*, 382–390. [[CrossRef](#)]
110. Domańska, U.; Wlazło, M. Separation of ethylbenzene/styrene systems using ionic liquids in ternary LLE. *J. Chem. Thermodyn.* **2016**, *103*, 76–85. [[CrossRef](#)]
111. Wlazło, M.; Domańska, U. Gamma infinity data for the separation of butan-1-ol-water mixtures using ionic liquid. *Sep. Purif. Technol.* **2016**, *162*, 162–170. [[CrossRef](#)]
112. Domańska, U.; Wlazło, M.; Karpińska, M.; Zawadzki, M. Highly efficient water/butan-1-ol separation on investigation of limiting activity coefficients with [P<sub>8,8,8</sub>][NTf<sub>2</sub>] ionic liquid. *Fluid Phase Equilib.* **2017**, *449*, 1–9. [[CrossRef](#)]
113. Wlazło, M.; Karpińska, M.; Domańska, U. Separation of water/butan-1-ol mixtures based on limiting activity coefficients with phosphonium-based ionic liquid. *J. Chem. Thermodyn.* **2017**, *113*, 183–191. [[CrossRef](#)]
114. Marciniak, A.; Wlazło, M. Activity coefficients at infinite dilution and physicochemical properties for organic solutes and water in the ionic liquid trihexyl-tetradecyl-phosphonium tricyanomethanide. *J. Chem. Thermodyn.* **2018**, *120*, 72–78. [[CrossRef](#)]

115. Wlazło, M.; Marciniak, A.; Zawadzki, M.; Dudkiewicz, B. Activity coefficients at infinite dilution and physicochemical properties for organic solutes and water in the ionic liquid 4-(3-hydroxypropyl)-4-methylmorpholinium bis(trifluoromethylsulfonyl)-amide. *J. Chem. Thermodyn.* **2015**, *86*, 154–161. [[CrossRef](#)]
116. Everett, D.H. Effect of gas imperfection in GLC measurements: E refined method for determining activity coefficients and second virial coefficients. *Trans. Faraday Soc.* **1965**, *61*, 1637–1645. [[CrossRef](#)]
117. Cruickshank, A.J.B.; Gainey, B.W.; Hicks, C.P.; Letcher, T.M.; Moody, R.W.; Young, C.L. Gas-liquid chromatographic determination of cross-term second virial coefficients using glycerol. Benzene + nitrogen and benzene + carbon dioxide at 50 °C. *Trans. Faraday Soc.* **1969**, *65*, 1014–1031. [[CrossRef](#)]
118. Design Institute for Physical Properties, Sponsored by AIChE (2005; 2008; 2009; 2010). Dippr Project 801—Full Version. Design Institute for Physical Property Research/Aiche. Available online: [http://knovel.com/web/portal/browse/display?\\_ext\\_knovel\\_display\\_bookid=1187&verticalid=0](http://knovel.com/web/portal/browse/display?_ext_knovel_display_bookid=1187&verticalid=0) (accessed on 12 April 2019).
119. Poling, B.E.; Prausnitz, J.M. *Properties of Gases and Liquids*; McGraw-Hill Publishing: New York, NY, USA, 2001. Available online: <http://lib.myilibrary.com?ID=91317> (accessed on 12 April 2019).
120. Domańska, U.; Królikowska, M.; Acree, W.E., Jr.; Baker, G.A. Activity coefficients at infinite dilution measurements for organic solutes and water in the ionic liquid 1-ethyl-3-methylimidazolium tetracyanoborate. *J. Chem. Thermodyn.* **2011**, *43*, 1050–1057. [[CrossRef](#)]
121. Grant, D.W. *Gas-Liquid Chromatography*; van Nostrand Reinhold: London, UK, 1971.
122. Domańska, U.; Laskowska, M. Measurements of activity coefficients at infinite dilution of aliphatic and aromatic hydrocarbons, alcohols, thiophene, tetrahydrofuran, MTBE, and water in ionic liquid [BMIM][SCN] using GLC. *J. Chem. Thermodyn.* **2009**, *41*, 645–650. [[CrossRef](#)]
123. Martins, M.A.R.; Coutinho, J.A.P.; Pinho, S.P.; Domańska, U. Measurements of activity coefficients at infinite dilution of organic solutes and water on polar imidazolium-based ionic liquids. *J. Chem. Thermodyn.* **2015**, *91*, 194–203. [[CrossRef](#)]
124. Ge, M.-L.; Deng, X.-M.; Zhang, L.-H.; Chen, J.-Y.; Xiong, J.-M.; Li, W.-H. Activity coefficients at infinite dilution of organic solutes in the ionic liquid 1-butyl-3-methylimidazolium methyl sulfate. *J. Chem. Thermodyn.* **2014**, *77*, 7–13. [[CrossRef](#)]
125. Zhou, Q.; Wang, L.-S. Activity Coefficients at Infinite Dilution of Alkanes, Alkenes, and Alkyl Benzenes in 1-Butyl-3-methylimidazolium Tetrafluoroborate Using Gas-Liquid Chromatography. *J. Chem. Eng. Data* **2006**, *51*, 1698–1701. [[CrossRef](#)]
126. Zhu, J.; Yu, Y.; Chen, J.; Fei, W. Measurement of activity coefficients at infinite dilution for hydrocarbons in imidazolium-based ionic liquids and QSPR model. *Front. Chem. Eng. China* **2007**, *1*, 190–194. [[CrossRef](#)]
127. Królikowski, M.; Królikowska, M. The study of activity coefficients at infinite dilution for organic solutes and water in 1-butyl-4-methylpyridinium dicyanamide, [B<sup>4</sup>MPy][DCA] using GLC. *J. Chem. Thermodyn.* **2014**, *68*, 138–144. [[CrossRef](#)]
128. Padászyński, K. An overview of the performance of the COSMO-RS approach in predicting the activity coefficients of molecular solutes in ionic liquids and derived properties at infinite dilution. *Phys. Chem. Chem. Phys.* **2017**, *19*, 11835–11850. [[CrossRef](#)] [[PubMed](#)]
129. Padászyński, K. Extensive Evaluation of the Conductor-like Screening Model for Real Solvents Method in Predicting Liquid–Liquid Equilibria in Ternary Systems of Ionic Liquids with Molecular Compounds. *J. Phys. Chem. B* **2018**, *122*, 4016–4028. [[CrossRef](#)]
130. Padászyński, K.; Domańska, U. COSMO-RS screening for ionic liquid to be applied in extraction of 2-phenylethanol from aqueous solutions. *J. Mol. Liq.* **2018**, *271*, 305–312. [[CrossRef](#)]
131. Ahlrichs, R.; Bar, M.; Haser, M.; Horn, H.; Kolmel, C. Electronic structure calculations on workstation computers: The program system turbomole. *Chem. Phys. Lett.* **1989**, *162*, 165–169. [[CrossRef](#)]
132. *MarvinSketch, Version 16.3.28, Release 2016*; ChemAxon Ltd.: Budapest, Hungary, 2016.
133. Becke, A.D. Density-functional exchange-energy approximation with correct asymptotic behaviour. *Phys. Rev. A* **1988**, *38*, 3098–3107. [[CrossRef](#)]
134. Perdew, J.P. Density-functional approximation for the correlation energy of the inhomogeneous electron gas. *Phys. Rev. B* **1986**, *33*, 8822. [[CrossRef](#)]
135. Schafer, A.; Huber, C.; Ahlrichs, R. Fully optimized contracted Gaussian basis sets of triple zeta valence quality for atoms Li to Kr. *J. Chem. Phys.* **1994**, *100*, 5829–5835. [[CrossRef](#)]

136. Domańska, U.; Lukoshko, E.V.; Królikowski, M. Separation of thiophene from heptane with ionic liquids. *J. Chem. Thermodyn.* **2013**, *61*, 126–131. [[CrossRef](#)]
137. Padaszyński, K.; Królikowski, M.; Zawadzki, M.; Orzeł, P. Computer-aided molecular design of new task-specific ionic liquids for extractive desulfurization of gasoline. *ACS Sustain. Chem. Eng.* **2017**, *5*, 9032–9042. [[CrossRef](#)]
138. Maginn, E.J. Molecular simulation of ionic liquids: Current status and future opportunities. *J. Phys. Condens. Matter* **2009**, *21*, 373101–373113. [[CrossRef](#)]
139. Smiatek, J. Aqueous ionic liquids and their effects on protein structures: An overview on recent theoretical and experimental results. *J. Phys. Condens. Matter* **2017**, *29*, 233001–233009. [[CrossRef](#)]
140. Shah, J.K.; Maginn, E.J. *Molecular Simulation of Ionic Liquids: Where We Are and the Path Forward. Ionic Liquids Further, Un COILED: Critical Experts Overview*; Plechkova, N.V., Seddon, K.R., Eds.; Wiley Online Library: Hoboken, NJ, USA, 2014; Chapter 6.
141. Gong, Z.; Sun, H. Extension of TEAM Force-Field Database to Ionic Liquids. *J. Chem. Eng. Data* **2019**. [[CrossRef](#)]



© 2019 by the author. Licensee MDPI, Basel, Switzerland. This article is an open access article distributed under the terms and conditions of the Creative Commons Attribution (CC BY) license (<http://creativecommons.org/licenses/by/4.0/>).